FATIMA

FArming Tools for external nutrient Inputs and water MAnagement

D2.2.4 Methodology for EO-assisted maps of nutrient requirements and of yield

WP2.2 EO for monitoring plant status and yield

André Chanzy, Martine Guerif, Frédéric Bourdin (INRA),

Alfonso Callera, Isidro Campos, José González-Piqueras, Julio Villodre; Sergio Sánchez, Jaime Campoy, Anna Osann (UCLM)

Horacio López; Francisco Jara (ITAP), María Calera; Nuria Jiménez, Vicente Bodas (Aliara)

Rosario Napoli, Claudia di Bene, Roberta Farina (CREA)

Guido d'Urso, Carlo Michele (ARIESPACE SRL)

Francesco Vuolo (BOKU)

Stamatis Stamatiadis (GNHM), Nicholas Dercas(AUA), Nicos Spyropoulos (SIGMA)

Petr Fucik (VUMOP)

European Commission | Horizon 2020 European Union funding for Research & Innovation

This project has received funding from the European Union's Horizon 2020 research and innovation programme under grant agreement No 633945.

Document Information

Grant Agreement	633945	**Acronym**	FATIMA		
Full Title of Project	Farming Tools for external nutrient inputs and water Management				
Horizon 2020 Call	SFS-02a-2014: External nutrient inputs (Research and innovation Action)				
Start Date	1 March 2015	Duration	36 months		
Project website	www.fatima-h2020.eu				
Document URL	(insert URL if document is publicly available online)				
REA Project Officer	Arantza Uriarte				
Project Coordinator	Anna Osann				
Deliverable	D2.2.4 Methodology for EO-assisted maps of nutrient requirements and of yield				
Work Package	WP – activity 2				
Date of Delivery	Contractual	M34	Actual	28/02/2018	
Nature	Other	Dissemination Level	PU		
Lead Beneficiary	INRA				
Lead Authors	André Chanzy	Email	Ande.chanzy@inra.fr		
Contributions from	UCLM, BOKU, CREA, UAU, Aliara, ITAP, BOKU, GNHM, DRAXIS, VUMOP				
Internal Reviewer 1	Jose González				
Internal Reviewer 2					
Objective of document	Description of the Nitrogen recommendation schemes based on EO information and evaluation across sites				
Readership/Distribution	All FATIMA Regional Teams; All WP leaders and other FATIMA team members; European Commission / REA; Public				
Keywords	Sentinel 2, satellite, Nitrogen fertilization, variable rate, heterogeneity,				

Document History

Version	Issue Date	Stage	Changes	Contributor
Draft	15/11/2017			André Chancy
V01	13/12/2017		Contributions from co-authors	
V02	28/02/2018		Final version	

Disclaimer

Copyright

Executive summary

This document presents the spatialized recommendation methods of nitrogen (N) fertilization using satellite remote sensing measurements. The Sentinel 2 mission offers a great potential for improvement thanks to 1) high temporal repetitiveness which makes it possible to follow the vegetation during the critical stage revealing the soil / water / nitrogen interactions on the development of the vegetal cover and thus to appreciate the potential of production and the limiting factors, 2) its high spatial resolution (10m) which is adapted to the spatialized application scale of fertilizers and 3) an interesting spectral content for the characterization of the nitrogenous state of plants. Seven methods were developed and applied to the wheat fertilization. The methods are divided into two main approaches:

- the use of remote sensing to detect lack of N and then adapt the fertilization to compensate for such a deficiency. This hold for the method based on the sufficiency index as well as those based on NNI.
- The use of remote sensing to establish the yield potential and thus adapt the fertilization to match the actual needs. The evaluation of the yield potential was done either simply by integrating historical LAI data, by considering biomass production through the NDVI dynamic or by considering the source in yield potential variability explicitly (soil properties as the organic matter or the water storage capacity) using a crop model. In season procedures to adapt the yield potential according to the actual vegetation development using the existing satellite images were developed

Results have shown gain provided by the different method that can lead to economic benefit that can reach 70€/ha in area with a low potential. In a benchmarking exercise, several methods are applied on the same fields and evaluated using a crop model to simulate the different fertilization maps. The comparison has shown that the different rationale led to very different maps both in terms of spatial pattern and applied dose. The evaluation protocol looks relevant to analyze the methods. Extending such a benchmark to several sites and a wide range of possible climates is required to compare the methods and strengthen them.

Table of contents

List of tables

List of figures

1 Purpose of the document

This document aims to present the spatialized recommendation methods of nitrogen fertilization using satellite remote sensing measurements. The Sentinel 2 mission offers a great potential for improvement thanks to 1) high temporal repetitiveness which makes it possible to follow the vegetation during the critical stage revealing the soil / water / nitrogen interactions on the development of the vegetal cover and thus to appreciate the potential of production and the limiting factors, 2) its high spatial resolution (10m) which is adapted to the spatialized application scale of fertilizers and 3) an interesting spectral content for the characterization of the nitrogenous state of plants, thanks in particular to the bands in the red edge spectral domain. To take profit of such new potentialities, different groups in FATIMA have developed and tested methods. As the Sentinel images are freely available and all the processing chains to make spatial registration and atmospheric effect correction are now mature, transfer of the companies able to provide the service to the farmer would be possible at reasonable cost. This was already the case with the development made by UCLM and Ariespace. This document, present the rationale of those methods and the experiment done to assess their results in order to identify the adding value of variable rate application governed by remote sensing derived recommendation. At the end we will provide a comparison of the method to see how they differed in results and what would be the impact on agronomic and environmental indicators derived from a spatialized crop model.

2 Method Presentation

The methods presented below are mostly adapted for wheat (one case NNI-1 was developed for the tomato) and follow different principles:

- Adapting the fertilization during the course of crop growth by evaluating the nitrogen content at the time of the fertilization decision. This holds for the Sufficiency index and the NNI approaches. The rationale is to correct lack of nitrogen for reaching an expected yield potential.
- Using a yield potential map derived from remote sensing historical observation and provide a recommendation adapted to the expected yield
- Using a crop model to infer some soil spatial patterns explicitly by its inversion using satellite images and yield map. The crop model is then used during the course of the experiment to identify contextual spatial patterns (soil nitrogen content, crop installation). The recommendation is then make by considering a yield potential derived from crop model simulation that take both soil permanent characteristics and contextual patterns.

2.1 Recommendation based on a Sufficiency index approaches using the Holland-Schepers model

2.1.1 Rationale of the method and innovation

Interpreting leaf nitrogen (N) concentration or vegetation indices (VI) for the purpose of making N recommendation is difficult because these are affected by cultivar and growth stage differences, cropping history, previous manure applications and cultural practices. Sensor measurements are additionally

affected by leaf architecture and sensor/plant distance relationships. For these reasons, values need to be normalized to reference a situation that has received modestly excessive amounts of N fertilizer (Schepers et al. 1992, Peterson et al. 1993). When normalizing vegetation indices, the plant readings are divided by the reading from the reference plants. The resulting quotient was termed the ‘‘Sufficiency Index’’ (SI) and used to guide sensor-based in-season N fertilizer recommendations (Biggs et al. 2002).

$$SI = VI_{sensed\ crop} / VI_{reference} \quad (2.1)$$

where $VI_{sensed\ crop}$ is the vegetation index (or measurement) of the sensed crop, and $VI_{reference}$ is the vegetation index (or measurement) of the non-N limited crop.

2.1.1.1 The Virtual Reference concept to estimate $VI_{reference}$

Extending the normalization concept to whole-field situations that exhibit spatial variability, producers typically install one or more N-rich strips in their fields to use as the reference (Raun et al. 2010). An analytical approach termed as the ‘‘virtual reference’’ statistically characterizes plants that demonstrate a level of vigor that is comparable to those commonly found within an N-rich strip, but without having to actually apply extra N fertilizer (Holland and Schepers 2011). The virtual reference approach uses the sensors to monitor a portion of the existing crop that is intended to represent the range in crop vigor within the field and then statistically identifies plants that are deemed to be non-N limiting and thus comparable to many of those that might be found in an N-rich strip. The vegetation index value for these non-N limited plants is used as the reference when calculating the sufficiency index for plants in the remainder of the field as variable-rate N fertilizer is applied.

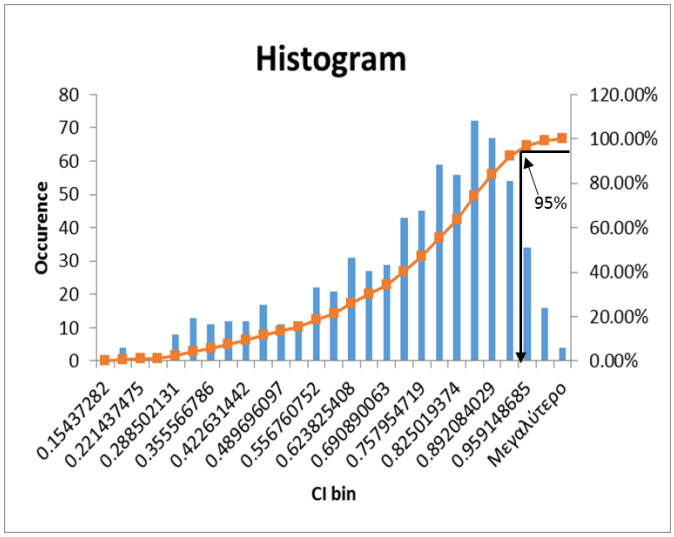

Figure 2-1. Sampled data distribution with cumulated percentile overlay for cotton at 70 days after planting in the Larisa pilot (2015). The 95-percentile value was used as the reference value of the Chlorophyll Index (CI).

During auto-calibration of the variable-rate system (Opt-N-Air) for on-the-go fertilizer applications in the Greek pilots, the 95-percentile value from a vegetation-index histogram of a representative crop row was used to determine the VI of adequately fertilized plants (Fig. 2.1). This value was used to calculate a sufficiency index value for other plants in the fields. The vegetation index of reference plants analyzed using an N-rich approach was 3–5 % lower than derived using the virtual-reference concept (Holland and Schepers 2011). When making maps of N requirement from satellite imagery, the VI histogram of the entire field can be used to derive the VI reference value.

2.1.1.2 The Holland-Schepers model for in-season N recommendation

The N application model involves directly inserting normalized sensor data (SI values) into a generalized plant growth function (Holland and Schepers 2010). Having access to reflectance data from three wavebands makes it possible to calculate SI values of several vegetation indices. We select NDVI (normalized difference vegetation index) for early-season growth conditions or NDRE (red-edge vegetation index) that is more responsive to crop N status under closed canopy conditions. NDRE is similar to the Chlorophyll Index that accurately estimates chlorophyll contents in contrasting species in terms of LAI, chlorophyll, canopy architecture and leaf structure for different crops (Gitelson et al., 2005). The simplest form of the model is when the back-off function to limit N application for low SI values is turned off:

$$N_{APP} = (N_{opt}) * \sqrt{\frac{(1 - SI)}{\Delta SI}} \quad (2.2)$$

N_{APP} is the N application rate and N_{opt} is the optimal in-season N rate to maximize crop yields. Embedded within N_{opt} are modifications to the soil N pool from processes that are difficult to quantify like mineralization, immobilization, denitrification, and leaching. SI is the sufficiency index (equation 1) and ΔSI is the sufficiency index difference parameter (ΔSI=0.3) for corn (Holland and Schepers 2010). When the back-off function is turned on to conserve N, the recommended N application rate increases as the SI decreases until the ΔSI threshold is reached, at which time the back-off function begins to reduce the N application rate (Fig. 2.2). This model has the mathematical form:

$$N_{APP} = (N_{opt}) * \sqrt{\frac{(1 - SI)}{\Delta SI * (1 + 0.1e^{m(SI_{thres} - SI)})}} \quad (2.3)$$

where the rate parameter m determines the rate at which the N application model decreases N supply and the SI threshold determines when the back-off function starts to limit N supply.

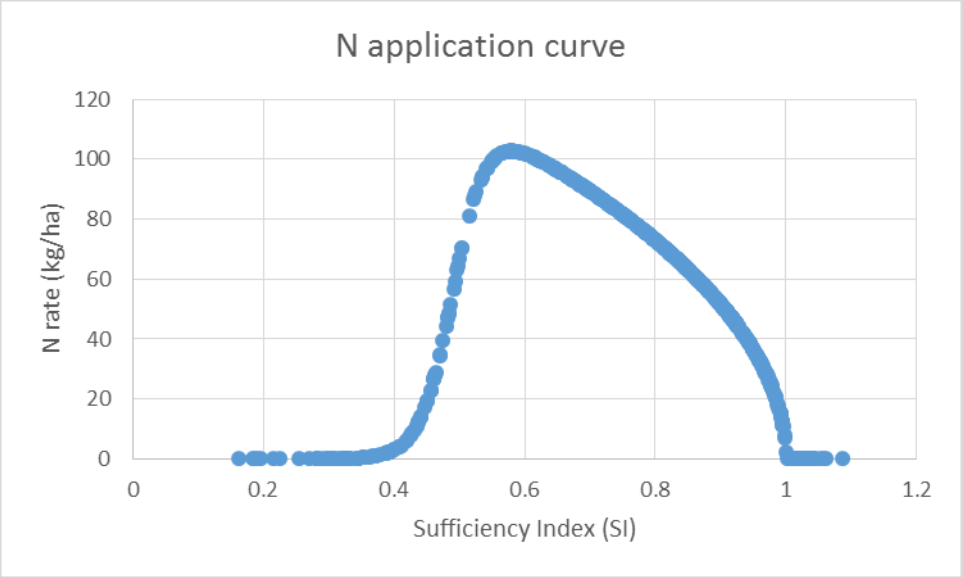

Figure 2-2. Recommended application rates using the N application model with the back-off function for irrigated cotton at 70 days after planting in the Larisa pilot (2015).

2.1.1.3 Implementation with S2 Satellite images

S2 datasets were obtained via ESA's Sentinels Scientific Data Hub (https://scihub.copernicus.eu/). The available products are in processing Level-1C, geometrically corrected and registered to the UTM 34N WGS84 ellipsoid with elevation correction applied. S2 images were acquired on March 2016. Digital image processing and analysis of the satellite data was carried out using SNAP (5.0, open source) software, while the manipulation of the spatial information was made using ArcGIS (10.3).

At the first pre-processing step, atmospheric correction was applied to convert the Top-of-Atmosphere reflectance values (TOA) of S2, to corrected Bottom-of-Atmosphere reflectance values (BOA). For the atmospheric correction, ESA's Sen2Cor plugin was used. Subsequently, bands 1, 9 and 10 were removed from the dataset. Then, the images were resampled in 10m resolution, using a bilinear method and were also subset to the study site extent. Then, a histogram stretch was made to enhance the radiometric resolution of the product.

At the processing phase, the Red Edge Normalized Difference Vegetation Index (RENDVI), was calculated, according to the following equation (2.4). RENDVI capitalizes on the sensitivity of the vegetation red edge to small changes in canopy foliage content, gap fraction, and senescence.

RENDVI= ((NIR-RE))/((NIR+RE)) 2.4

Where: NIR is the near-infrared band 8 and RE the Red Edge band 6

In our research we have tested also a modified form of RENDVI using as NIR the Red Edge band 7 and as RE the Red Edge band 5, called RENDVIm. The results and the comparison of the two RENDVI types show that RENDVIm performs more reliable results, closer to the results of ground data.

2.1.1.4 Comparison of ground sensor data to satellite imagery as input variables in the Holland-Schepers model

The Holland-Schepers model has been used successfully in ground-sensor VRA systems by delivering Economic Optimum N Rates in four field trials in the Greek pilot area (see Deliverable D3.1.4). However, the utility of the model to estimate spatially variable N requirement has not yet been verified with the use of satellite imagery. One step towards this direction is the comparison of degree of similarity between ground sensor and satellite maps of canopy reflectance using the red edge NDVI from which the sufficiency index is derived. The two sources of information are naturally differing in several ways. Here we present one case study comparing Crop Circle ground sensor measurements to World View 2 satellite imagery in one cotton field of the Thessaly plain.

The WV2 scenes were obtained from Space Imaging Munich, in bundle format, one 0.5m panchromatic channel and eight 2m multispectral channels, in 16-bit digital format. Initially, a histogram enhancement of the images was made and an atmospheric correction, utilizing Geomatica's ATCOR model, was applied. The Digital Number values of each WV2 image have been converted to Top of Atmosphere reflectance and then to surface reflectance. This procedure was fulfilled utilizing the Digital Elevation Model (DEM) of the area, geographic longitude/latitude and the weather conditions that were present at the time of image acquisition. These latter parameters were automatically calculated by importing the images through the suitable import algorithm. At the final pre-processing step, a precise co-registration of the images was made using ground control points of high accuracy, and resampling was made at 2m and 0,5m for multispectral and pansharpen images, accordingly.

At the processing stage, the Red Edge Normalized Difference Vegetation Index (RENDVI) was computed.Then, the RENDVI values of the images selected were manipulated in ArcGIS, in order to be compared with the Ground Data Values of RENDVI that derived from VRT sensor in the cotton field 2015, Greek pilot area (Figure 2.3). Initially, the images were clipped to each crop limits and then the sampling method was applied to extract every pixel value of the index .

For the statistical comparison of WV2 and VRT values of RENDVI, the Jaccard Index was utilized. The Jaccard index is a statistic, used for comparing the similarity and diversity of sample sets. The Jaccard coefficient measures similarity between finite sample sets, and is defined as the size of the intersection divided by the size of the union of the sample sets (equation 2.4b).

$$J(A,B) = \frac{|A \cap B|}{|A \cup B|} = \frac{|A \cap B|}{|A| + |B| - |A \cap B|}.$$

(If A and B are both empty, we define $J(A,B) = 1$.)

$$0 \leq J(A,B) \leq 1.$$

(2.4b)

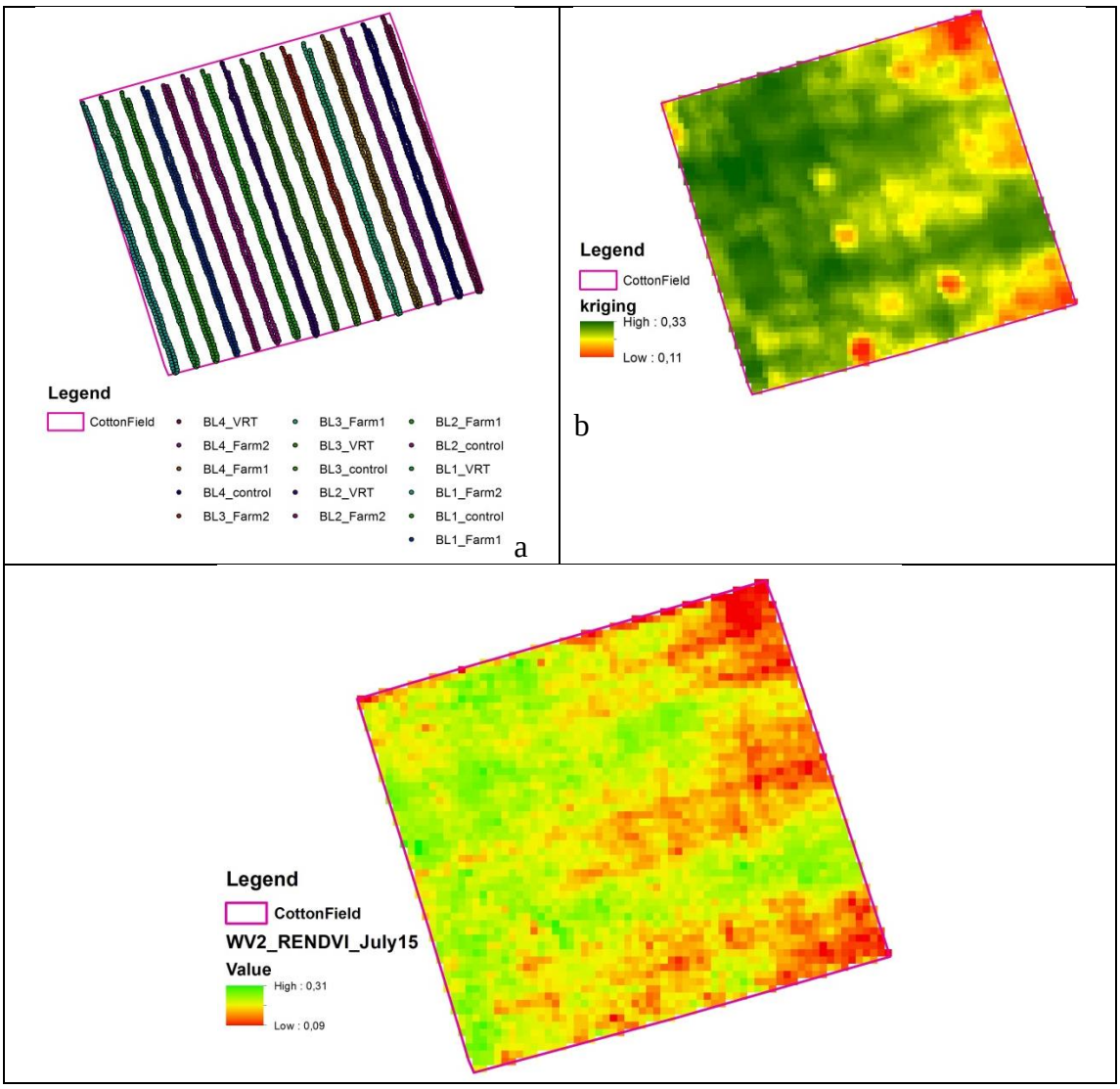

Figure 2-3. The RENDVI values of WV2 (bottom), and ground measurement (top)

According to this statistical comparison, as far as it concerns the cotton field of 2015 (Figures 2.3), the similarity of the WV2 and VRT sensor values, was approximately 84%. These results are very promising by considering that the actual pixel values are naturally differing from ground sensor measurements in terms

of degree of soil interference, spatial resolution, field and crop row coverage, reflectance penetration depth of the optics, wavebands of modulated vs natural light, analytical differences in the methods of map production, etc.

2.1.1.5 Fields delineated to management zones

Extending from entire fields to situations where the field has been delineated into discrete management zones, the model requires some type of scalar to adjust N rates according to the productivity of each zone. Processing of a Sentinel 2 image of the Remi site in Montpellier indicated that zone-specific N_{opt} values of N rates in 2016 were required to account for differences in yield potential. The cutback function of the model was only used for the low productivity zone to account for limited water availability and likely little plant response to N inputs. The pixel N rates estimated for each management zone using a universal RENDVI reference value of 0.38 are shown Fig. 2.4.

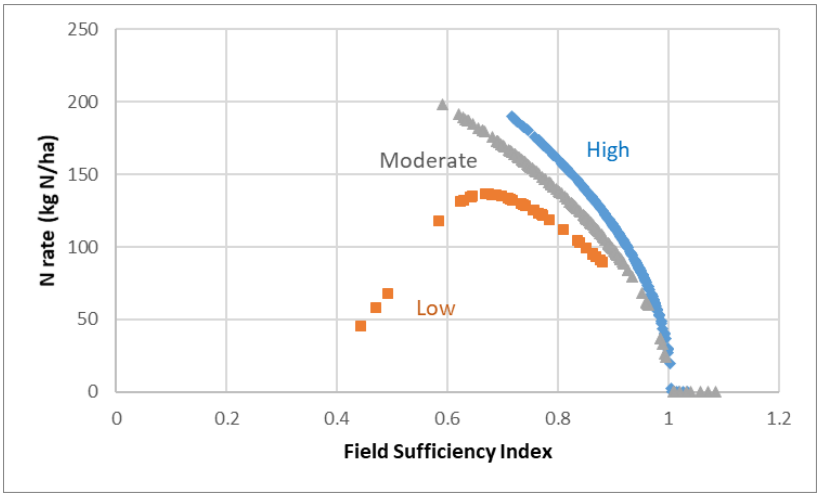

Figure 2-4. Recommended N application rates of three management zones using Sentinel 2 red edge NDVI values of the Remi wheat field in 2016.

2.1.2 Required inputs

In the case of processed satellite imagery, producing a map of N rates using the Holland-Schepers model requires the following parameters:

1. **Processed satellite imagery** for the RENDVI vegetation index
2. **RENDVI reference value**: Extraction of the 95-percentile value from the histogram of the pixels of the whole field. This value replaces $VI_{reference}$ in equation 2.1.
3. **Estimation of N_{opt}**: $N_{opt}=N_{total} - N_{pre}$ where N_{total} is the optimum total N rate to maximize crop yields and N_{pre} is the N already applied to the field prior to in-season application in kg/N/ha. In case that the value of N_{total} is not known or cannot be estimated from yield potential, the farmer-perceived total N rate is probably the only source of reliable information for a particular field.
4. **Use of the back-off function**: The last step before the application of the model is to decide if the back-off function is preferred to conserve N in problematic areas of the field where plants are unlikely to recover to their full yield potential. When the back-off function is used with an $SI_{threshold}$ of 0.7, a moderately fast cutback of m=20 will cut back to zero application at SI=0.2 and may suffice in most cases.

2.2 Recommendation base on NNI approaches -1

2.2.1 Rationale of the method and innovation

Definitions

The approach tested in the Italian case-study on wheat and tomato is based on the concept of the Nitrogen Nutrition Index NNI, defined as the ration Na/Nc between the actual crop N uptake (Na) and the critical N uptake (Nc), on the basis of the concepts expressed by Lemaire et al. (2008)

This methodology is based on the combined use of : i) crop growth models (EPIC applied in Tarquina, STICS in Tarascon) to derive the relationship between the Leaf Area Index (LAI) and the Dry Weight Biomass (W); ii) Sentinel-2 spectral indexes in the red-edge region to estimate canopy chlorophyll content and LAI.

Assessment of Nc

Nc is expressed by means of the following relationship:

$$Nc = a_c \, W^{-b} \qquad (2.5)$$

with W being the dry biomass in t/ha. Coefficients a_c and b for different crop species are given in [1].

For Wheat we have: $a_c = 5.3$; $b = 0.44$. For Tomato $a_c = 4.5$; $b = 0.33$

Calibrated simulation of EPIC based on the experimental data set of 2016 in Tarquinia, have been used to derive the dry weight biomass W as a function of LAI for each crop type. The following relationships have been found:

Wheat : $W\ (t/ha) = W\ (t/ha) = 0.433\ LAI\_S2^{1.64}$ ($R^2 = 0.997$) (2.6a)

$Nc = 5.3\ (0.433\ LAI\_S2^{1.64})^{-0.44}$

Tomato: $W\ (t/ha) = 1.2763\ LAI\_S2^{1.5237}$ ($R^2 = 0.998$) (2.6b)

$Nc = 4.5\ (1.2763\ LAI\_S2^{1.5237})^{-0.33}$

which can be applied considering LAI as estimated from Sentinel-2 data.

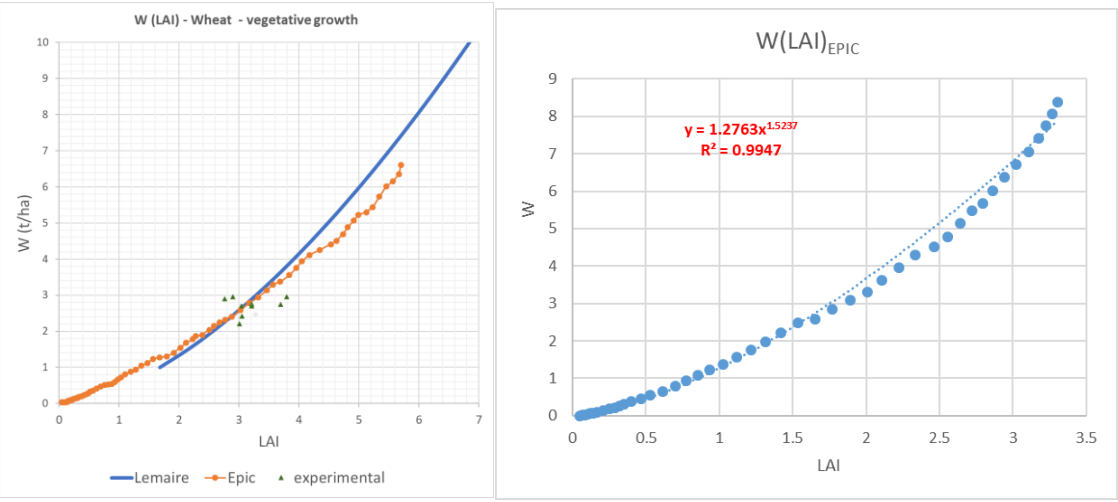

Figure 2-5. Calibration of W(LAI) relationship based on EPIC and field data – Wheat (left) and Tomato (right)

These relationships can be applied during the growth stage and not at the full maturity.

With the Tarascon data set, calibrated simulation of STICS based on the experimental data sets have been used to derive the dry weight biomass W as a function of GLAI. The following relationship has been found:

Wheat : W (t/ha) = GLAI (0.17*GLAI+0.91) 2.7

$Nc = 5.3\ [GLAI\ (0.17*GLAI+0.91)]^{-0.44}$

which can be applied considering GLAI as estimated from inversion of ProSail on the basis of drone reflectance data.

Assessment of Na in TArquina

By statistical analyses between observed MC-100 values and contemporary Sentinel-2 images the following relationship has been derived in the Tarquina site:

WHEAT: $(LAI\_S2 * Ch\_{MC100}) = 532.83\ CIred\_edge$ (R^2= 0.78 ; p<0.001) [mg/m^2] (2.8a)

TOMATO: $(LAI\_S2 * Ch\_{MC100}) = 507.58\ CIred\_edge$ (R^2= 0.80; p<0.001) [mg/m^2] (2.8b)

where *CIred_edge* is given by (B7/B5-1) with B5, B7 indicating Sentinel-2 surface reflectance (20 m spatial resolution).

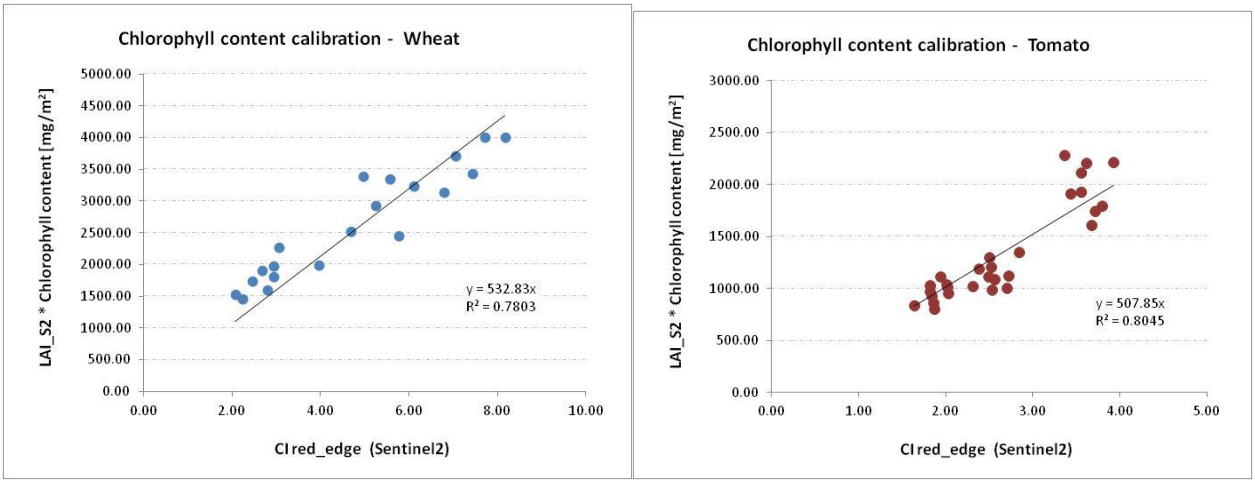

Figure 2-6. Calibration between CIred edge and canopy Chlorophyll content

The following calibration has been found from the Italian experimental data set in 2016 between Chlorophyll content measured by Apogee MC-100 and laboratory N%:

WHEAT: $N\% = 0.0055\ Chlorophyll\ content\_{MC100} + 0.6401$ (R^2= 0.3976) (2.9a)

TOMATO: $N\% = 0.004\ Chlorophyll\ content\_{MC100} + 2.4528$ (R^2= 0.7164) (2.9b)

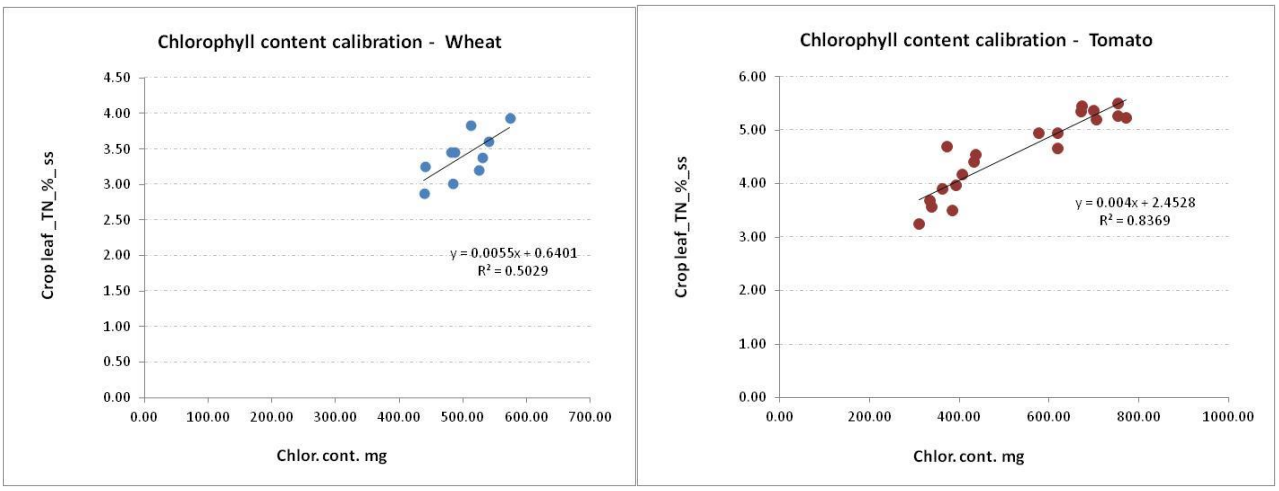

Figure 2-7. Calibration between laboratory N% and MC-100

Hence, Na is derived by combining Eqs. (2.8) and (2.9):

WHEAT: $Na = 0.0055 * (532.83\ CIred\_edge)/LAI\_S2 + 0.6401$ (2.10a)

TOMATO: $Na = 0.004 * (507.58\ CIred\_edge)/LAI\_S2 + 2.4528$ (2.10b)

Finally, the Nitrogen Nutrition Index NNI=Na/Nc is calculated as the ratio of Eqs.(2.10) and (2.7).

By statistical analyses between observed SPAD values and contemporary GLAI and CI_green (EO-based) the following relationship has been derived:

WHEAT: $(GLAI * SPAD) = 12.932\ CI\_green$ [µg/cm^2] (2.11)

Assessment of Na in Tarascon

The following calibration has been found from the experimental data between Chlorophyll content measured by SPAD and laboratory Na%:

$Na\% = 1.184\ SPAD - 8.375$ (R^2= 0.659) (2.12)

A conversion factor of 0.1 is needed to have mg/m^2. Hence:

WHEAT: $Na\% = 0.1184\ SPAD - 0.8375$ (R^2= 0.659) (2.13)

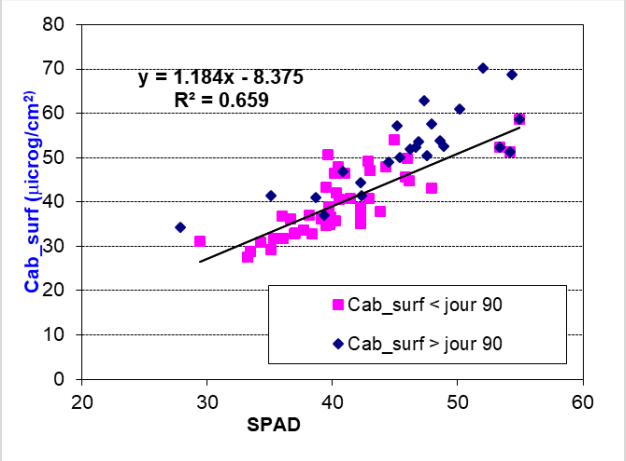

Figure 2-8. field relationship in Tarascon

Hence, Na is derived by combining Eqs. (2.8) and (2.9):

WHEAT: Na = 0.1184 * (12.932 *CI_green*)/GLAI -0.8375 (2.14)

Finally, the Nitrogen Nutrition Index NNI=Na/Nc is calculated as the ration of Eqs.(2.10) and (2.7).

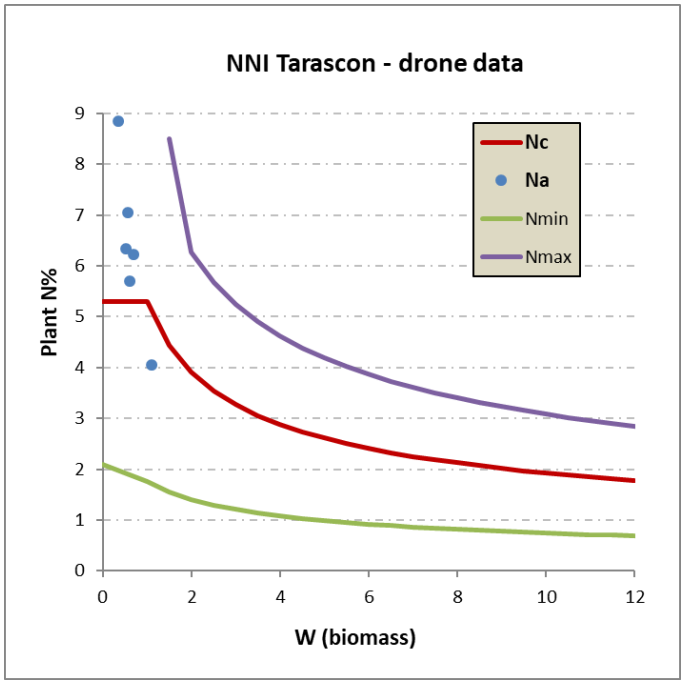

Figure 2-9. NNI computed with the Drone Data on Tarascon field

The NNI maps need to be coupled with a crop model in order to provide a quantitative indication for dosing fertilizers. Direct feedback about fertilization dosage based on NNI can be obtained in the case of processing tomatoes, where frequent fertirrigation applications are practiced. In this case, it would be also easier to modulate the concentration of fertilizer for different irrigation laterals.

2.3 Recommendation base on NNI approaches -2

2.3.1 Rationale of the method

The methodological framework selected is based on the concept of critical N concentration (Colnenne et al. 1998) to obtain the N recommendation via the N Nutrition Index (NNI) (Lemaire et al. 2008). This approach was originally based on ground measurements and recently tested and applied with remote sensing data by (Houles et al. 2007) and in a number of other studies (Cilia et al., 2014, Vouillot et al., 1998). The main limitation of the approach is the need for extensive calibration to estimate the two input parameters required for the application of the NNI: the above ground dry mass accumulation (W) and the actual N concentration (%Na) at a specific growing stage. Our aim was to apply the NNI approach, using an empirical relationship to derive dry mass accumulation from Leaf Area Index (LAI) and %Na from a spectral chlorophyll index (CI). The approach was applied to the experimental plot with winter wheat (Triticum aestivum) for 2016 and 2017.

Spectral vegetation indexes are traditionally used to estimate leaf chlorophyll concentration, which is related to N content (similarly to what the ground-based N-Tester is measuring) and to estimate LAI and

above ground dry mass accumulation. Potentially, one should use vegetation indexes, or more sophisticated approaches, that are able to decouple the effect of one vegetation variable (e.g. leaf chlorophyll) from another (e.g. leaf area index) to maximize the information content. To estimate %Na, we tested empirical relationships between ground measurements of plant N and the Double-peak Canopy Nitrogen Index (DCNI) (Chen et al. 2010). For dry mass, we used a time series of Sentinel-2 LAI data cumulate during the crop growing season.

2.3.2 Required inputs

The method requires remote sensing derived products for LAI and %Na. Concerning the latter empirical relationship are needed.

2.4 Recommendation based on Yield potential Approaches

2.4.1 Rationale of the method

The practice of fertilization requires:

- ✓ Planning the amount of N requirements to apply and its scheduling for the next campaign. It requires a prognostic tool prior to the growth season.
- ✓ Adjusting the timing and amount of N supply to the actual crop growth and N status. It requires an in-season diagnostic tool. This diagnostic tool should enable us the fine-tuning of N supply according the actual crop development.

The EO-based yield potential here shortly described tackle both aspects above mentioned. The classical "point" approach relates external N input calculation, and its application scheduling during the growing season, according the expected or goal yield. Then the N fertilizer recommendation is back-calculated from the yield goal by assuming typical grain protein content and a grain N/total N uptake ratio, and further assuming some level of N use efficiency, and finally giving credit for other N sources (e.g., previous legume crops, manure, N mineralization, and N in irrigation water). This approach uses a “mass balance” concept for the N balance, running jointly with a water balance, both in the root soil layer, where N crop uptake, N soil and atmospheric processes are taken in account to establish the optimum amount of N supply and its scheduling. This classical “yield potential approach” doesn´t account for the within-field yield variability because of inherent spatial differences in fertility levels and water availability (Holland and Schepers, 2010).

The EO-based yield potential approach follows the classical procedure, taking advantage of accumulated scientific knowledge, but considering each pixel, the minimum unit of information able to capture within-field heterogeneity, as the target to apply the soil N water balance plus the soil water balance.

2.4.1.1 Pre-season N recommendation

The key is to establish the spatial distribution of the expected yield, which will be the yield target map for each field. The Figure 2.10 shows the flow diagram for this procedure. Time series of multispectral imagery is the key for obtaining the yield target map. In a first approach, this EO-based yield target map should be similar in its concept to the map obtained from ground yield monitoring by using appropriate devices mounted on the harvest machinery. Furthermore, biomass accumulation during the growing cycle also is able to obtain by exploiting the information from the time trajectory for each pixel, which provided by the time series of multispectral imagery.

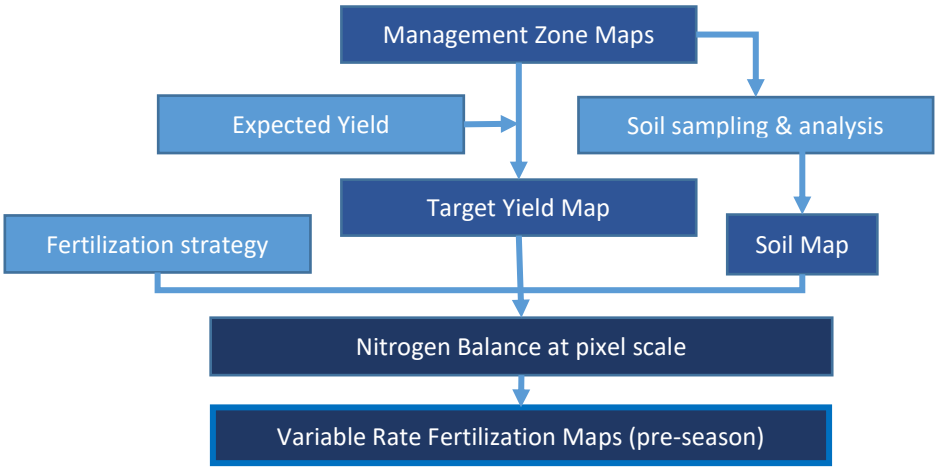

Figure 2-10. Flow diagram of the elaboration of the VR fertilization maps in pre-season.

2.4.1.1.1 Mapping within-field biomass

All of the current crop growth models rely on two basic processes that explain vegetation growth. These basic processes happen in the soil-plant-atmosphere system and explain the biomass accumulation as the result of transpiration and solar radiation captured by plants. The basic assumption is that the rate of biomass accumulation is driven by actual transpiration, T, and light absorbed, APAR, being the minimum rate of both processes what determines the current biomass accumulation, what is expressed according to the Equation 2.15

$$B = min[\int WP\ T\ dt;\ \int \epsilon\ APAR\ Ks\ dt] \quad (2.15)$$

- B: biomass accumulated in a time t per unit of surface [kg/m^2]
- WP : water productivity [kg of biomass / m^3 of water transpired]; crop dependent
- ε: conversion efficiency of solar radiation into biomass or ratio of chemical energy equivalent of absorbed PAR [kg/MJ]; crop depending
- APAR, absorbed PAR [MJ/m^2]
- Ks: water stress coefficient [dimensionless]. It requires a soil water balance in the root soil layer
- T, actual transpiration [m^3 water transpired/m^2]

On the described conceptual basis, we implement a direct remote sensing-based approach for monitoring biomass growth, with the aim to be operational. This approach integrates directly time series of multispectral imagery into the above described vegetation growth modelling, WP and LUE. Details about this procedure can be found in Campos et al. (2018). The experience gained during the FATIMA project encourages these methods for the assessment of the biomass production in several crops, including wheat, corn and soybean. The ongoing analyses showed promising results in garlic, onion and sugar beet.

2.4.1.1.2 Mapping yield. Addressing the impact of water and N stresses

Grain yield production is strongly related with the biomass production although not in an unequivocally way. The crop yield can be estimated as a variable proportion of total aboveground biomass that goes into the harvestable parts depending on the biotic and abiotic stresses, the duration, the severity and the crop physiological stage during the stress period. This proportion is known as harvest index (HI). The reduction in grain yield from stresses occurs because of the reduction of assimilate production during grain filling (Ritchie et al., 1998).

Whereas transpiration or APAR provide a suitable base for mapping potential biomass production, no comparably, simple and functional methods have been developed for the assessment of HI using

exclusively EO and meteorological data. However, we have implemented an EO-based approach for the HI estimation, following the existing knowledge according the approach proposed by Sadras and Connor (1991) and reanalyzed by Kemanian et al. (2007). This method is based on the ratio between biomass accumulation after anthesis over the biomass accumulation during the entire growing cycle, this ratio is named θ_B in this work. The HI vs θ_B relationship is not linear and can be described by an increasing function, see Equation 2.3.2. The values of HI estimated by the function are limited by the maximum HI attainable for the specie (HI_x) and the minimum HI obtained in source limited conditions (HI_0).

$$HI = HI_x - (HI_x - HI_0) \cdot exp(-k \cdot \theta_B) \quad (2.16)$$

Therefore, the developed EO-based approach of HI relies on the estimation of θ_B at pixel scale, by using the procedure for biomass growth during the whole growth cycle above described.

Addressing the impact of water and N stresses

Water and N stresses impact on the biomass accumulation, by lowering the potential biomass growth rate. Yield decreasing reflects both the decrease on biomass and the decrease on HI. Active ongoing research we are dedicating to understand how the EO-based models above described are able to capture the impact of both type of stresses and its influence in terms of within-field variability. Simplified operational approach requires as input the knowledge of the obtained average yield.

2.4.1.1.3 Mapping potential soil productivity. The Management Zones Map

We can define potential soil productivity as the attainable yield for a crop on each point of the soil in a determined field under standard weather and management, mainly irrigation and nutrient practices. Mapping potential soil productivity describes within-field yield variability in terms of soil fertility for a fixed crop. The Management Zones Map, MZM, is the final representation of this soil fertility for a fixed crop under standard weather and management.

The developed approach for obtaining MZM requires the use of multiannual EO time series. For each campaign, crop and management we can obtain the spatial distribution of biomass and yield. Our finding show similar spatial pattern across years, discarding areas with abnormal crop developments irrigation or fertilization fails, bad crop installation, pests or diseases, etc.. Although uniform management is a usual practice, we strongly recommend a careful inspection, including farmer consultation, discarding the effect of the management in the crop development.

2.4.1.2 In season Diagnostic Tool: Fine-tuning of N supply

Once crop development starts, timing and amount of N supply could need adjustment of the previous planning according with the actual crop N status and its actual growth. The in-season diagnostic tool should enable us the fine-tuning of N supply according the actual crop development. As described, planned N requirements maps are based on an expected yield map, which means a determined expected crop growth and development in each elementary unit of the information map. By using crop phenology stages, the timing of application naturally adjusts to current crop-soil-weather conditions. Models based on degree-days or accumulated reference evapotranspiration can help to situate the date for the key stages.

The in-season EO-based monitoring of current crop status and its spatial distribution should indicate if the target yield can be achieved or if it needs some adjustment. Anomalies in crop development refers when current crop development differs from expected in each management unit of the field. Anomalies detection requires comparison of spatial distribution of current crop development and that considered as standard for each elementary unit of the field. The source and scope of so EO-detected anomalies needs to be

identified usually by field inspection, because a set of causes can occur. Bad crop establishment, floods, drought, rodent attacks, and others, occurring in early crop development stages and lowering the number of fertile plants, can jeopardize seriously the yield, at least for the affected areas. So the planned N application in these areas must be modified according the produced damage. For N deficit detection, and so fine-tuning the amount of N to apply, we have implemented the EO-based Nitrogen Nutrition Index NNI. The flow diagram of this procedure showed in the Figure 2.11.

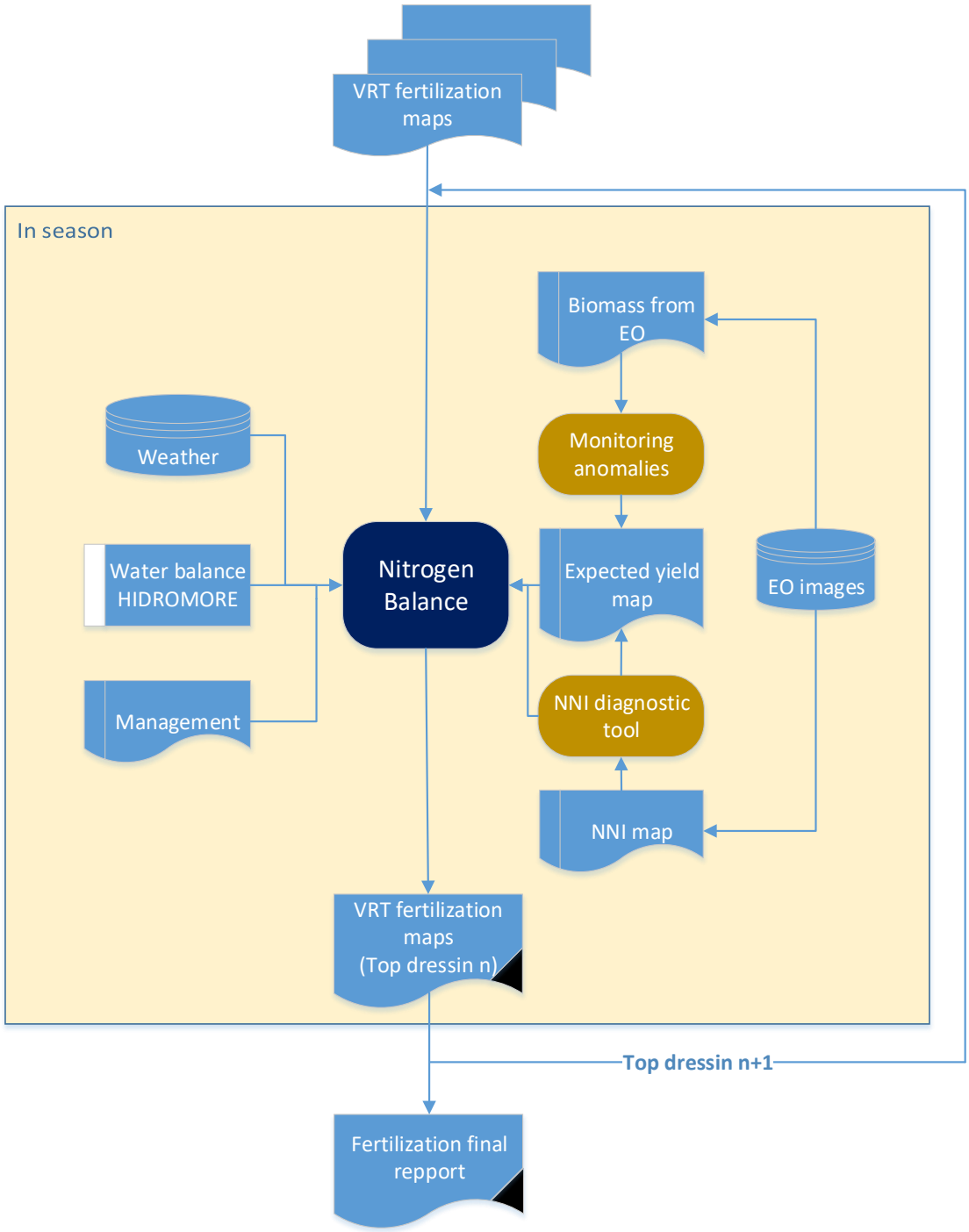

Figure 2-11. Flow diagram of the elaboration of the VR fertilization maps in season.

The EO-based Nitrogen Nutrition Index

The Nitrogen Nutrition Index, NNI (Justes et al., 1997) (see 2.2.1). Here we considered that

$$\%Na = \frac{QNa}{B} \quad (2.17)$$

where

- *QNa* Nitrogen content of canopy cover [kgN/m^2]
- *B* Dry Biomass [kgN/kg$_{dry\ biomass}$]

The decline of critical plant concentration *%Nc* is related with crop biomass, ***B*** according a generalized equation, described by Eq. 2.18 (Justes et al., 1997) where *A* and m are parameters depending on the crop :

$$\%Nc = A.B^{-m} \quad (2.18)$$

Combining the equations 3, 4 and 5 we obtain the relationship between the NNI and the crop biomass and N content (see Eq. 6)

$$NNI = \frac{\left({}^{QNa}/_{B}\right).100}{A.B^{-m}} \quad (2.19)$$

As Eq. 2.19 points, NNI computing requires both the estimation of *QNa* and biomass; We assume we can estimate *QNa* from spectral vegetation indices, being selected those based on the reflectance in the red edge bands. A common linear relationship between QNa and a red edge-based index is showed in the Eq. 2.20

$$QNa = m * MTCI + b \quad (2.20)$$

where:

MTCI MERIS Terrestrial Chlorophyll index (Dash & Curran, 2004) computed by using the spectral bands, 6,5 and 4 of Sentinel2A and Sentinel 2B imagery.

On the other hand, biomass can be estimated from remote sensing by integrating time series of multispectral images into the crop growth models., as was described in Eq. 2.3.1. Setting a threshold value for NNI parameter below which the protocol activates. At present, for wheat the NNI value has been set at 0.90, although more experience is required. For other crops, this threshold will be set in the future.

The way to proceed when a NNI deficit activates a warning should be:

1. **Discard false positive** (artifacts by clouds or other atmospheric effects)

2. **Field inspection** looking for diseases, weeds, failure of irrigation system and/or fertilization application, and soil/plant sampling.

    a) Use the Nitrogen&Water Balance to confirm or not the deficit.

    b) If sampled soil N doesn´t match with NB, adjust the NB to the sampled soil N

3. **Making decision**

    a) If actual N_{min} is known **to recalculate the NB** and proceed accordingly.

    b) According **NNI value , calculate $QN_d = Qn_{act} - QN_c$** and apply

2.4.2 Required inputs for the EO-based yield potential

2.4.2.1 Inputs required for Pre-season N recommendation:

Management Zones Map.

✓ Time series of EO images describing the growing cycle. Several campaign(s) in number enough for extracting common spatial pattern and removing/discarding management impacts

✓ Average yield, ancillary data

✓ Weather: reference evapotranspiration ETo, Incident Solar Radiation Rsi, Precipitation

✓ If expected water stress occurring during the growing cycle (rainfed crops) Crop Phenology. Dates about Sowing date; Crop Emergency and flowering. MZM elaboration requires mapping of root soil water holding as an intermediate step.

Additional inputs required for Simplified N balance

✓ Organic matter and initial mineral N_{ini} soil content (field representative data, sampling areas are indicated by the MZM)

✓ Farmer current local practices: amount of N applied, type, number and scheduling of N application

A simplified practical procedure was adopted when spatial soil data are not available or are very limited. In this case, the MZM enables mapping Nuptake, by transforming the yield target map into N crop uptake, assuming a typical grain protein content and a grain N/total N uptake ratio. Then, our practice seems to suggest as best option to distribute the amount of N proportional to the estimated Nuptake. Previous knowledge of yield when known N fixed doses has been used in previous campaign can provide some type of information about the soil contribution by inverting the N balance, contributing to refine the average N requirement and its spatial distribution.

2.4.2.2 Inputs required for NNI monitoring and anomalies detection

✓ Time series EO images in real time + previous campaigns

✓ Weather, ETo, Rsi, Precipitation

2.5 Recommendation based on yield potential (2)

2.5.1 Method rationale and innovation

For the Czech pilot (Dehtare), field trials (1 field block, 25 ha in 2016 and five field blocks) were delineated based on soil conditions (soil survey, repeatedly analyzed soil samples) and farm management for cereals (spreader width, tramlines shape, etc.). Crop yield potential was assessed based on the multi-temporal satellite data. As the main data source, ESPA repository of LANDSAT 5 and 8 satellite images was used, which offers surface reflectance products, main vegetation indices (NDVI, EVI – reflecting crop biomass) and clouds identification by CFmask algorithm. A selection of scenes from recent 8 years was made for the specific farm area to collect cloud-free data related to the second half of the vegetation period. Yield

potential was calculated for separate scenes as the relation of each pixel to mean EVI value of the whole field. In the next step, all scenes were combined and median value for each pixel was calculated as the yield potential value. Due to the spatial resolution of Landsat data (30 m per pixel), the final map was smoothed by kriging interpolation into a spatial resolution of 5 m per pixel (Fig. 2.12). Calculation of yield potential was further enhanced by available Sentinel 2A/B images in 10-m spatial resolution.

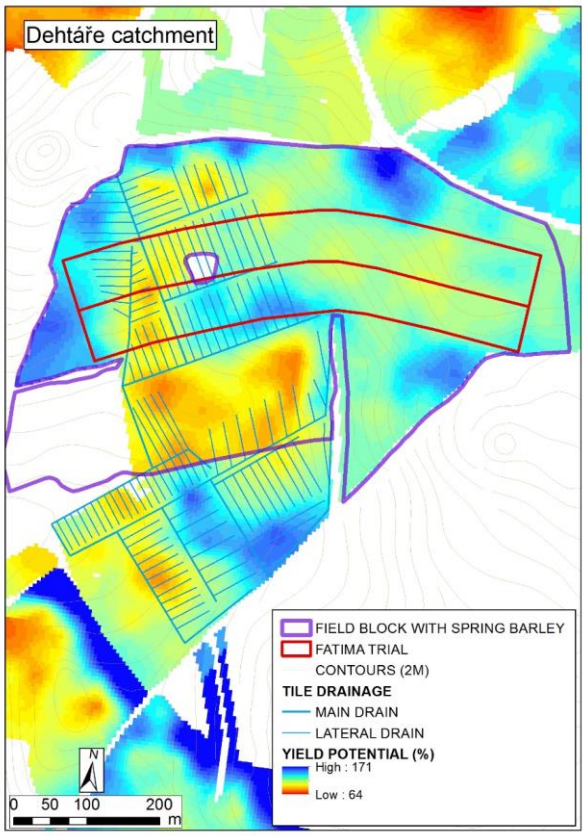

Figure 2-12. Yield potential for Dehtáře pilot site (Kojcice farm), Czech Rep. (trial 2016)

Based on this as well as on a detailed soil survey and repeated soil sampling (mineral N content), variable fertilizer application zones (70 – 120%) were delineated. of the site (65%) was fertilized uniformly (UNI trial). The VAR and UNI trial differed in 2016 and 2017,

The rationale of the method was to follow the yield potential (YP); i.e. to put less N fertilizers where the YP is low, and, for setting the N doses, taking into account also the actual crop status and soil N min content.

2.6 Recommendation based on yield potential (3)

2.6.1 Method rationale and innovation

Farmers regularly compile their own nitrogen (N) budget to obtain N prescriptions. This process is based on various information, e.g. regulations (legal limits and best practices), field measurements and crop management strategies. Once they decide on the amount of N fertiliser to apply, we provide the spatial variability of plant growth to more efficiently allocate fertiliser (in space). The rational of the method is to spatially optimize the prescribed N amounts (calculated by Farmers) knowing the application ranges (minimum and maximum). This approach does not “require a calibration to be carried out in a representative area of the field before work can begin” as for similar approaches based on sensors mounted on the tractor (e.g. N-Sensor Yara, GreenSeeker). A number of yield potential maps (all derived

from Sentinel-2 LAI data at different temporal aggregations) are available to monitor the spatial variability and the decision rule for selecting the most appropriate is described in Figure 2.13.

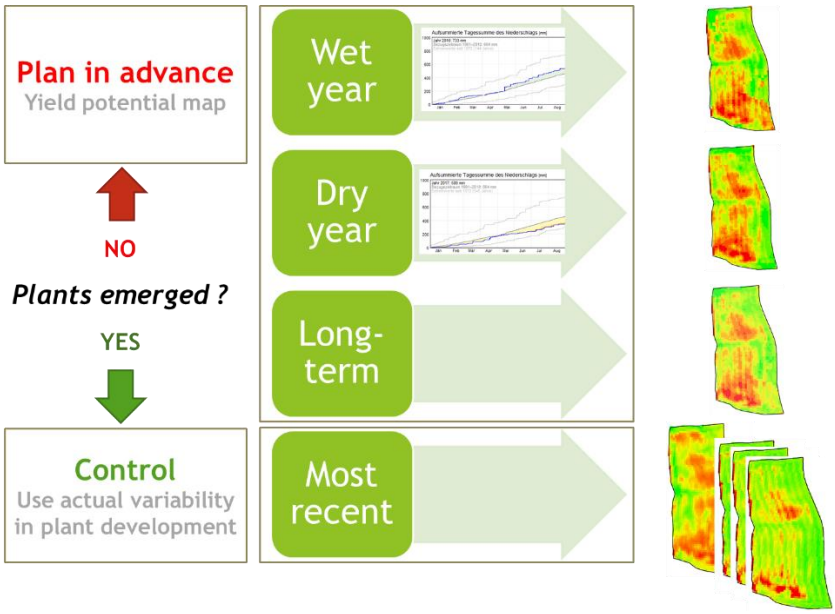

Figure 2-13. Decision rule for the selection of the Yield Potential Map.

2.6.2 Requires inputs

We require time series of Sentinel-2 data to regularly monitor the crop development and to produce maps of yield potential at different temporal scales (Figure 2.14).

We also require the N application ranges (minimum and maximum values from the on-farm N prescription) and the management strategy. Two fertilization strategies are possible: "Catch-up" will allocate more N fertiliser where there is less potential for vegetation growth and this is generally used with the first or second application. Farmers can also decide to apply more N fertiliser where there is more vegetation growth. This approach is called "Top-up". A graphical user interface (Figure 2.14) is available for providing these inputs and for producing the outputs (N application maps in shapefile format).

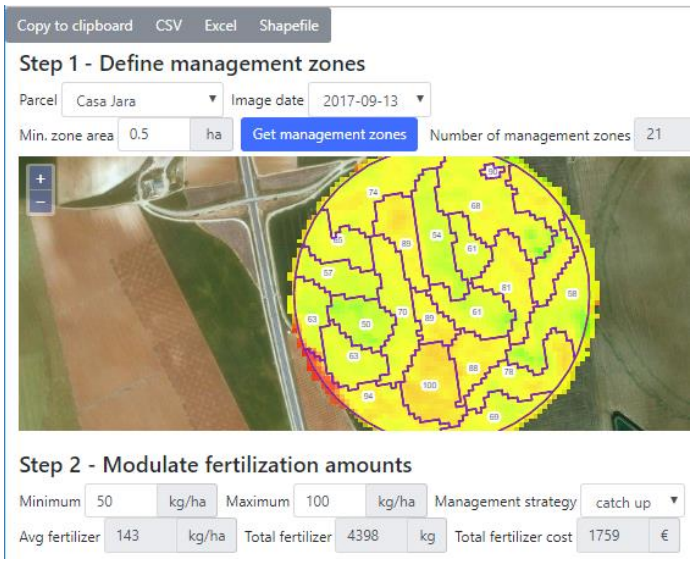

Figure 2-14. Graphical user interface for generating Variable Rate Application maps

2.7 Recommendation based on the use of crop model (STICS)

The Objective of the method is to give a spatial recommendation for the 2nd and 3rd Nitrogen supply on a wheat field. The approach can be extended to other crops that can be simulated by the STICS model as barley, sunflower, corn or rape.

2.7.1 Rationale of the method and innovation

The approach is based on a combination of a crop model – the STICS model (Brisson et al., 1998) – and spatialized data (satellite data, yield maps) to understand and reproduce spatial variability in a given cropped field, allowing a subsequent adaptation of nitrogen fertilization (Houlès et al., 2005).

The method involves data assimilation techniques such as model inversion procedures to retrieve input parameters values from the comparison between simulations and observations of a subset of STICS output variables (Figure 2.15).

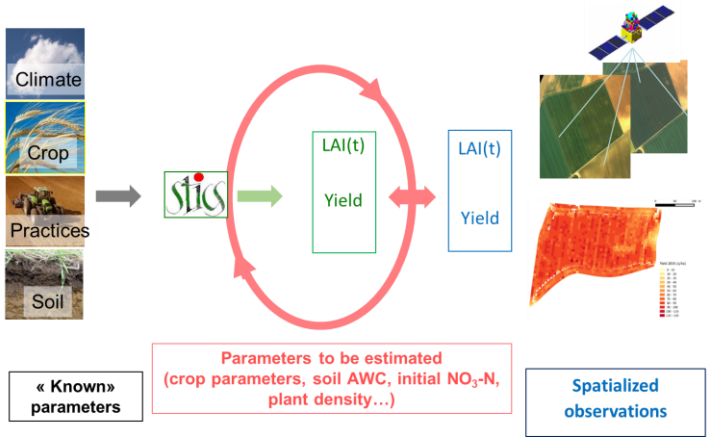

Figure 2-15. Principles of crop model inversion procedures for the estimation of a given set of parameters

The calculation of the fertilizer N recommendation is a 3 steps approach (Figure 2.16) where:

- historical data (climate, yield maps…) are used to parameterize the crop variety of interest within STICS and to estimate some permanent soil properties;
- early-season remote-sensing data, in the year we wish to make a fertilizer N recommendation, are used to assess crop status and soil initial N conditions;
- fertilizer N recommendation is calculated at the decision time.

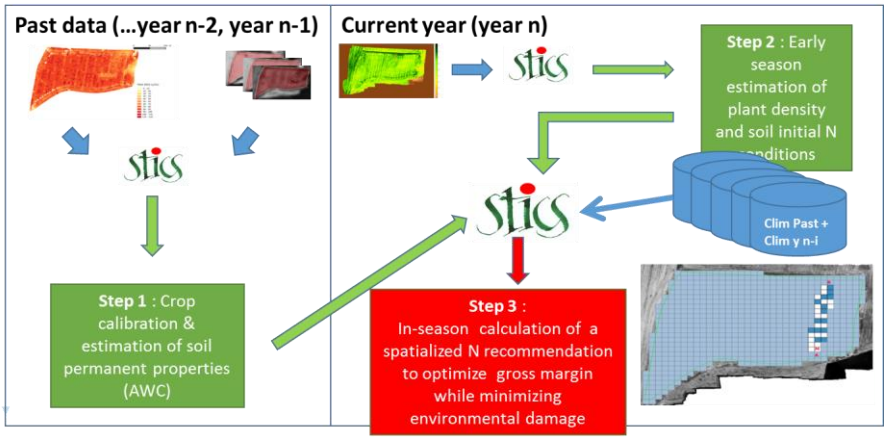

Figure 2-16. Schematic view of the INRA 3 steps approach

2.7.1.1 Step 1: Estimation of crop variety parameters and soil water storage capacity

Crop growth and yield formation in STICS are driven by the nitrogen and water availability in the soil, as well as the ability for the crop to utilize those resources for its development throughout the growing season. Such drivers are controlled by the mineral nitrogen and water content in the soil at the start of the simulation, some permanent soil properties (texture, depth…), climate, crop management, and crop variety-related genetic parameters (e.g. temperature sums, biomass growth-related parameters, water stress sensitivity…). As a consequence, a good parameterization of the STICS soil and crop components is necessary for an accurate diagnostic of the vegetation state at the decision time and the subsequent calculation of the fertilizer N recommendation.

In the operational context of the FATIMA project, only the information collected from the farmer (crop management, yield maps, soil analyses…) or easily available from external sources (satellite data, climatic data, soil maps…) could be used to parameterize STICS. Therefore, with only limited available data, the objective was rather to improve the parameterization of an existing default STICS variety, by adjusting a subset of STICS crop parameters, than to run a full calibration procedure.

During the lifespan of the FATIMA project, the crop-variety calibration protocol was developed and tested sequentially as follows on several bread wheat (*Triticum aestivum* L. *subsp. aestivum*) and durum wheat (*Triticum turgidum* L. *subsp. durum* (Desf.) Husn.):

1. First, existing default STICS varieties were screened to identify the one that better matched observations of leaf area index (LAI) dynamics and yields. The selected variety was used as a starting point for the calibration procedure.
2. A sensibility analysis was carried on to identify a limited subset of crop variety-related STICS parameters to be modified in order to improve the selected default STICS variety.
3. The calibration phase *stricto sensu* was run following an inversion procedure, based on the Simplex method from the Optimistics software (Buis et al., 2011), which allowed the estimation of a subset of parameters from LAI, yield and plant nitrogen observations.
4. The new parameterized wheat variety was validated on independent model simulation units (Figure 2.17).

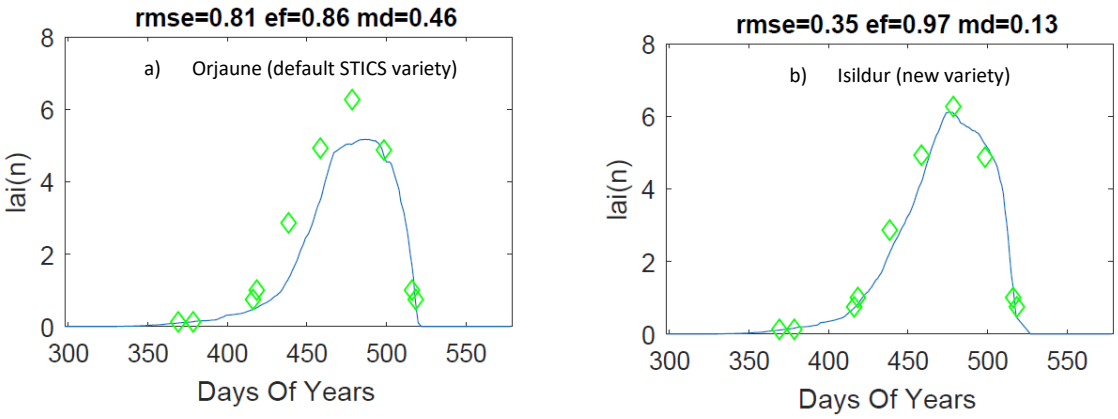

Figure 2-17. Example of an improvement of the simulation of LAI dynamics with a newly parameterized Durum wheat variety. Sentinel 2-derived LAI observations are given by the green diamond-shaped symbols while simulated LAI values are represented with the blue lines.

Permanent soil properties within STICS can be either set as default values, calculated directly from field measurements (texture, chemical composition, bulk density…), or estimated following an inversion procedure on field observations (LAI dynamics, yield maps), as proposed by Varella et al. (2010) for the estimation of soil water storage capacity and depth. In this project, the GLUE (Generalized Likelihood Uncertainty Estimation) method (Guerif, 2007) was used to estimate the spatial distribution of the soil water storage capacity, on several pilot sites, from satellite-derived (SPOT 5, Sentinel 2) LAI time-series and yield maps. An example of outputs from such method is given in Figure 2.18.

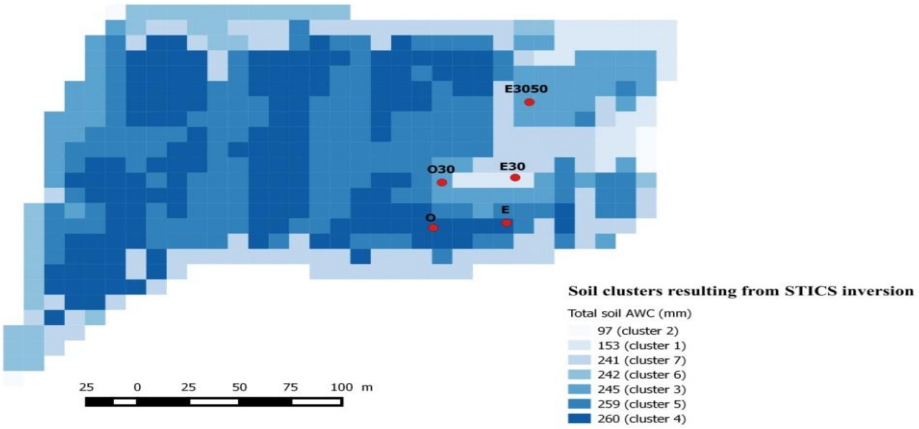

Figure 2-18. Soil map showing the 7 soil clusters identified from the inversion of yield and remote-sensing data on the Tarascon field (France) during the 2014-2015 growing season. For each cluster, soil available water content (AWC) was calculated using outputs from the STICS inversion.

2.7.1.2 Step 2: Diagnostic of the crop status at the decision time

Once the parameterization of the soil and plant components are completed within STICS, using data from previous years, the initial soil mineral N content and the quality of the crop installation must

be assessed as they may have a strong impact on the amount of fertilizer N required at a given time to achieve targeted yields while minimizing detrimental environmental impacts.

In the present approach, early-season remote-sensing-derived LAI information was used to invert the STICS model and retrieve spatially-distributed plant densities and soil mineral N content at the start of the season. Simulated plant densities were usually within the range of densities observed in field plots. The inversion procedure was similar to the one described in the previous section and was performed for each homogeneous group.

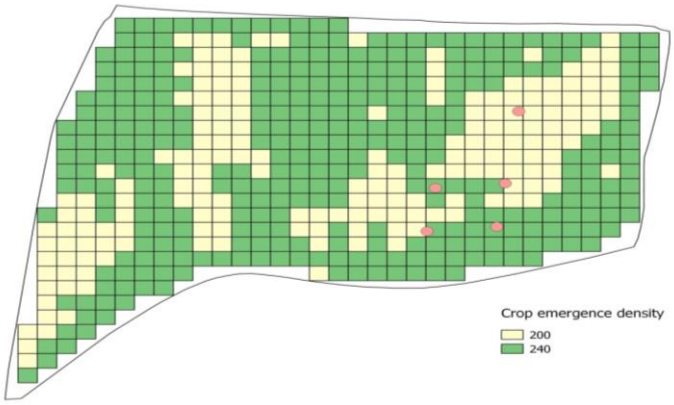

Figure 2-19. Plant density map showing the 2 homogeneous groups identified from the inversion of early-season Sentinel 2-derived LAI data on the Tarascon field (France) during the 2015-2016 growing season.

2.7.1.3 Step 3: Fertilizer N recommendation at the decision time

An agro-environmental criterion, based on agronomic (e.g. yield, protein content) and environmental (e.g. soil mineral N content at harvest) simulation results, was used to determine the variable N fertilizer rates. Such criterion was optimized using the STICS crop model over a set of scenarios combining variable fertilizer N doses and various climatic predictions. Observed weather data were used to simulate the crop development until the day of the recommendation, while 30 years of historical weather data (1984-2013, SAFRAN data base) were used to predict weather data until harvest. Fertilizer N doses to be applied were selected so that the farmer's gross income could be maximized under the constraint of a 20 kg N ha^{-1} threshold for the residual soil mineral N content after harvest.

2.7.2 Required data

Historical data: yield map, LAI temporal series covering the whole crop cycle. Early data are required to address the crop installation quality whereas data at the end of the cycles is very important to characterize the soil water storage capacity.

Leaf Area index from remote sensing product during the diagnostic phase before nitrogen applications (2^{nd} and 3^{rd})

Agricultural practices: Previous crop, previous crop residue management, tillage, sowing date and density, plant variety, Nitrogen fertilization calendar and supply

Soil properties: organic matter, initial guess for soil hydraulic properties (texture data) and soil depth

Daily meteorological data: These data must include precipitation and required data to compute potential evapotranspiration (radiations, air temperature (min and max), Air water vapour pressure, wind velocity). Those data has to cover :

Data before the time of the decision including a warming period before sowing

historical data (ideally 30 years). When those data are not available, reanalysis can be used (as the SAFRAN product distributed by meteoFrance)

2.7.3 Innovation with respect to current practices

Among the current commercial solutions distributed to the farmers that provide N fertilization maps from remotely sensed images, we should mention the Farmstar product for modulating the 3rd N fertilizer application on winter wheat (http://www.farmstar-conseil.fr/en/our-offer/modulation/) which is available since the early 2000s. Its concept is based on a mixed approach between NNI assessment and crop model approach.

An evaluation of the crop biomass and amount of N absorbed by the crop is done from remote sensing images (historically Spot and airborne measurements and now Sentinel2) at the moment when the recommendation has to be made (near the end of the stem elongation stage); from those values, projections are made with simple models of the crop biomass and the nitrate that will be provided by soil organic matter mineralization at the date of flowering; the recommendation of N dosis to bring through fertilization in order to lead the crop at an optimal N status at this date is therefore calculated. A lot of ground measurements databases are used to calibrate the models and make the recommendation robust.

However, some limitations of the method do exist: no account for the soil status (nitrogen and water), nor for the yield potential linked to soil available water capacity AWC nor for their within-field variability. And above all, because it was conceived in the early 2000s, it uses very few remote sensing information (a sole date).

Our method presents several advantages as compared to this reference method:

- It uses as many images as are available in the context of Sentinel2 offer, allowing a very precise evaluation of the time evolution of the crop behavior and of the crop N needs;
- Thanks to the possible assimilation of numerous images into the crop model, it estimates the variability of the quality of crop establishment, the remaining nitrate in the soil and the yield potential linked to soil AWC, allowing a potentially more precise site specific representation of the crop growth and estimation of the N needs.
- The use of a dynamic crop model simulating the whole crop-soil system (and future climate scenarios) for estimating optimal doses allows to take account not only of crop performances criteria but also of environmental constraints. Even if such constraints are not actually written in the legislation, this method may become fully relevant in case they are enacted.

3 Evaluation methods

The evaluation of each method was done by conducting field measurements (part 3.1). The aim was to validate the basic information used to recommend fertilization and in some case, a real test of nitrogen fertilization spatial recommendation. The latter remains delicate because the control of the actual nitrogen dose made on the plot is poorly known when the modulation areas are small. In addition, we conducted a benchmarking exercise of the recommendation methods (part 3.2). Since we did not have a field factorial test that allowed us to cross fertilization recommendations with production potential, we used crop models (STICS, EPIC) to build a spatial simulator to compare the different recommendations. . The simulator was deployed on 3 plots (Tarascon field , INRA SFT field and DEHESA 2015 field) presenting significant and known soil heterogeneities. The crop model allows, for each nitrogen fertilization recommendation, producing agronomic (yield, protein content, nitrogen use efficiency) or environmental (nitrogen leaching, nitrogen balance at the end) indicators. This deliverable is limited to the presentation of the results on the Tarascon field on which the exercise was completed. Its deployment on other sites will be necessary for a scientific valorisation of this work.

3.1 Evaluation through VRT experiment

3.1.1 SI approach : Experimental design and treatments

Experimental fields were divided into four blocks and three treatments were randomly assigned within each block to follow a randomized complete block design (Fig. 3.1). Each treatment was a field strip of several rows wide running the entire length of the field to simulate full-scale field conditions, to encompass variability of soil properties and to accommodate the operation of the variable-rate applicator and harvester. The three treatments consisted of a control with pre-plant application only, a farmer pre-plant and in-season uniform N application and a pre-plant with in-season variable-rate application (VRA). A field strip without any pre-plant or in-season N application was also included whenever possible. The VRA applicator delivered in-season VRA and uniform farmer applications of granular ammonium nitrate (34.5-0-0) on the soil surface of each treatment strip (see deliverable D3.1.1). In-season monitoring of soil properties and crop nutrient status took place from 1 m^2 sub-plots in three landscape positions of each treatment strip shown in Fig. 3.1. Ten composite leaf samples were taken from each plot before and/or after VRA application of fertilizer. Grain yield was measured from sub-plots at harvest and representative grain samples were taken for laboratory analysis. Grain yield was also measured for the entire treatment strips using a harvester.

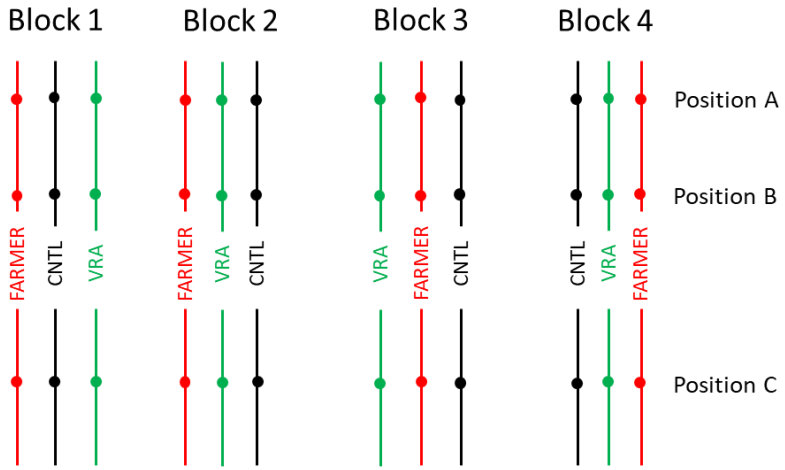

Figure 3-1. Generalized experimental design of pilot fields in Greece. Lines represent treatment strips (Farmer: farmer practice, Cntl: preplant control, VRA: variable-rate application) and circles the position of plots.

3.1.2 NNI approach-1

The procedure outlined above has been defined by using the experimental dataset of Tarquinia (Fava farm) acquired during the growing season 2016, and it has been validated by using independent measurements during 2017. Sentinel-2 Chlorophyll Index based on the red-edge band has been used to estimate the canopy chlorophyll content, which resulting values was compared with field measurements (MC-100) on the same date of satellite pass. The results of the validation are summarized in the plots below, which confirm that the calibration is transferable.

Successively, the calculation of NNI has been carried out by using the equations described in Section 2.2.1

3.1.3 NNI Approach-2

The original NNI approach was first applied with ground-based measurements of dry mass and %N performed during the growing season at different points in time. It was qualitative evaluated by visually inspecting the results against the experimental Nitrogen Dilution Curve that was derived using the approach described in (Lemaire et al., 2008, eq.(2) and coefficients indicated in Table 3.1 for wheat).

Using the ground data, empirical relationships were established between W and LAI and between %N and DCNI. The NNI was calculated and the maps were visually assessed for spatial consistency and correspondence between NNI levels and known N rates of the experimental plots.

3.1.4 Yield potential approach

3.1.4.1 Biomass production based on the temporal series of multispectral EO images

One of the main task developed during the project FATIMA by the IDR-UCLM group was the evaluation of the capability of temporal series of multispectral images combined with available meteorological data to provide, along the entire growing cycle, the key variables into the models based on water and light use efficiency for biomass estimation. The analysis performed were presented in a paper

published in a scientific journal (Campos et al., 2018) and this paragraph summarize the experiments oriented to the evaluation of the methodology. The specific objectives were the estimation of the parameters LUE and WUE for wheat based on the proposed approach and the evaluation of the three models under field conditions for the assessment of biomass. A similar analysis analyzing the aptitudes of this approach for the assessment of yield and biomass in maize and soybean was published by members of the IDR-UCLM group in the course of the project (I Campos et al., 2017).

The calibration dataset was obtained in three fields located in Albacete (South-East of Spain). These fields (Field 1, 2 and 3) were monitored in 2015 and 2016 during the spring wheat growing cycle, from January to July. The validation dataset was comprised of three fields (fields 4, 5 and 7). Fields 4 and 5 were located in Albacete and were monitored in 2015 during the spring wheat growing cycle. The datasets for the fields 1 to 5 were obtained in the frame of the project FATIMA. Field 7 is located in Ponca City, OK (north-central Oklahoma, USA) and was monitored during the winter wheat growing cycles in 1998-1999 and 1999-2000 (AmeriFlux site designation: US-Pon). For additional information about the fields monitored the reader is referred to the Table 3.1. Considering the objectives of this analysis, the validation and calibration datasets were in sharp contrast with respect to location, varieties, stresses, management practices and climate. No nitrogen or water deficit was detected in the field 1, 2 and 3 while the field 4 and 5 were under water and/or nitrogen deficits. Field 7 was winter wheat planted in a different climatic conditions, and these factors guarantee the differences in those variable related with the meteorological conditions during the growing cycle. For a broad description of the input data, ground data of biomass used for calibration and validation and the core measurements performed in the fields the reader is referred to Campos et al. (2018).

Table 3-1. Coordinates, irrigation and fertilization doses in the calibration and validation sites.

Fied ID	Year monitored	Managemet	Variety	Irrigation mm	Fertilization, Kg (N, P, K)	Yield (t/ha)	Coordinates
1	2015 CJ	Irrigated, direct seeding	Califa	452	(257, 81; 65) 5 doses	9.22	39.25º N 1.99º W
2	2016 DL	Irrigated, conventional	Califa	580	(294, 129; 55) 5 doses	9.41	39.13º N 2.91º W
3	2016 LG	Irrigated, conventional	Califa	461	(349, 132; 165) 6 doses	10.10	38.89º N 1.87º W
4	2015 CM	Irrigated, direct seeding	Galera	230	(140, 79; 0) 3 doses	3.84	39.08º N 1.66º W
5	2015 DL	Irrigated, conventional	Califa	447	(268, 120; 150) 6 doses	7.06	38.87º N 1.84º W
6	2016 CJ	Irrigated, direct seeding	Califa	453	(218; 105; 34)	7.51	39.0632; -1.6752
7	98-99	Rainfed, conventional	AsegCo 2174	-	(88; 26; 0) 1 dose	NA	36.77º N 97.15º W
7	99-00	Rainfed, conventional	AsegCo 2174	-	(88; 26; 0) 1 dose	NA	36.77º N 97.15º W
8	2016 FR	Rainfed, conventional		-	(-)	6	

3.1.4.2 Maps of within-field variability of yield production

An additional analysis was the assessment of crop growth variability at the scale of commercial farm. The proposed approach integrates time series of spectral vegetation indices into the crop growth models as proposed for the estimation of biomass production but is centered in the assessment of the spatial variability. The methodology was applied in commercial fields planted with wheat and managed in irrigated

conditions, the fields monitored are the fields 1, 2, 4 and 6 already described in the **Erreur ! Source du renvoi introuvable.**. The performance of the proposed approach was evaluated analyzing the variability estimated by the model versus the variability based on the yield maps obtained by combined-mounted grain yield monitors. For a broad description of the methodology the reader is referred to Campos et al. (2017).

The spatial distribution of the harvestable yield was mapped using a combined-mounted grain yield monitor (Trimble CFX750). The measurements of the yield monitor were calibrated against the total production weighted every 3-4 ha and the out-layers detected at the beginning and the final of the segments were removed manually. For the quantitative analysis of the yield maps, the yield data (points) were averaged at the scale of 3 by 3 pixels. For the comparison of the results of the model and the ground measurements of biomass, the values calculated by the model were averaged in 1 ha around the measurement locations. For the comparison with the yield maps, the values calculated by the model and based on the yield maps were averaged for an area equivalent to 3 by 3 pixels of the satellite images used in the model. In both cases, the field data were compared with the yield and biomass estimated by the model at grain maturity.

3.1.4.3 Evaluation of the variable rate fertilization trials

The objective is the comparison of the crop performance managed under homogeneous doses, following the farmer´s management, and under variable rate fertilization (VR). The hypothesis behind the experimental design is that the application of the VR can optimize the use of nitrogen promoting the land productivity in terms of yield and nitrogen uptake. The experiment was carry out in commercial fields, where the homogeneous and the VR can be applied using the conventional machinery. For the evaluation of the variable rate fertilization precognition, the methodology was applied and evaluated during two consecutive campaigns the fields 1 (2015) and 2 (2016), see Table 3.2.

Each field was divided in different zones with well demonstrated differences in the potential productivity based on the temporal evolution of the spectral vegetation index NDVI for the previous campaigns (see figure 3.2). The N requirements of each zone was estimated following the N balance approach described before for an average yield of 10000 Kg/ha in 2015 and 9000 Kg/ha in 2016. In 2015 the VRF was applied varying the N doses applied during the initial crop development according with the expected productivity (locations 1, 2 and 3 in the Figure 3.2). These locations compound the positive VR treatment (VR+). The reference in the field was obtained applying the average N dose in locations with high and low expected productivity (locations 4 and 5 in the Figure 3.2). These locations compound the homogeneous treatment (Hom). Finally, the doses were inverted with respect to the expected productivity (locations 6 and 7 in the Figure 3.2). These locations compound the inverse VR treatment (VR-). In 2016 only the VR+ and Hom. treatments were implemented, and the expected yield was revised according to the experience gained. The regular management limited the application of VRF during latter crop stages because the N species used after tillering are mainly N solution applied with the irrigation water. The total doses applied in each location are presented in the Table 3.2.

The results were analyzed in terms of average yield obtained in each treatment, the nitrogen extracted in the grain production, the nitrogen harvest index and the weight of grain obtained for each unit of N applied. The ground data used for the calculation of the indicator was obtained by means of samples (measurements of grain yield and the N content at grain maturity). The samples were collected manually in pre-selected measurement locations (see Figure 3.2).

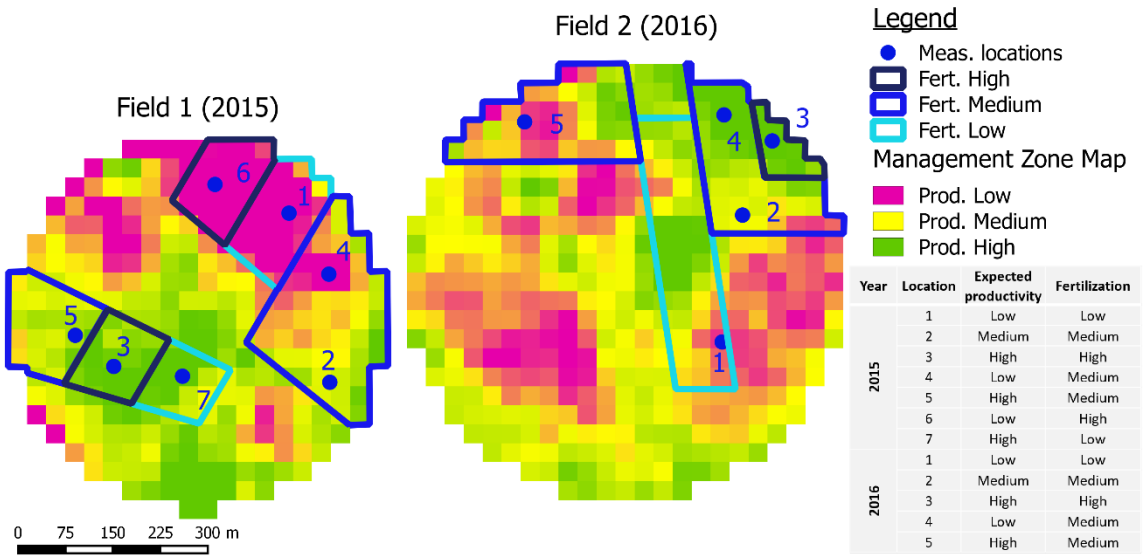

Year	Location	Expected productivity	Fertilization
2015	1	Low	Low
	2	Medium	Medium
	3	High	High
	4	Low	Medium
	5	High	Medium
	6	Low	High
	7	High	Low
2016	1	Low	Low
	2	Medium	Medium
	3	High	High
	4	Low	Medium
	5	High	Medium

Figure 3-2. Maps of management zones for the fields 1 and 2 where the variable fertilization based on the potential productivity was evaluated.

Table 3-2. Summary of the N fertilization, expected productivity, actual yield and N exported in each location in both analyzed campaigns.

Growing season	Location	Expected productivity	Fertilization (Kg N/ha)	Yield (T/ha)	N uptake. (Kg/ha)
2015	**1**	Low (8.5 T/ha)	211	9.03	238
	2	Medium (10 T/ha)	257	8.36	220
	3	High (11.5 T/ha)	303	10.20	282
	4	Low (8.5 T/ha)	257	9.27	247
	5	High (11.5 T/ha)	257	8.57	222
	6	Low (8.5 T/ha)	303	9.66	270
	7	High (11.5 T/ha)	211	9.49	247
2016	**1**	Low (8.0 T/ha)	167	6.51	172
	2	Medium (9.0 T/ha)	218	7.22	209
	3	High (10.0 T/ha)	257	9.02	274
	4	Low (8.0 T/ha)	218	6.95	198
	5	High (10.0 T/ha)	218	7.58	222

3.1.5 Yield potential approach (2)

The VAR trial on 35% of the site was used to evaluate the recommendation. Mineral fertilizers were distributed accordingly with GPS operated spreader three times from early April to late May. The rest of the site (65%) was fertilized uniformly (UNI trial). The VAR and UNI trial differed in 2016 and 2017,

The rationale of the method was to follow the yield potential (YP); i.e. to put less N fertilizers where the YP is low, and, for setting the N doses, taking into account also the actual crop status and soil N min content. However, within the experiment, areas with low YP were fertilized also by higher N amounts and vice versa.

Ground monitoring of spectral characteristics for spring barley was done in Dehtáře by two offline hand devices; Yara N-tester and GreenSeeker. N-tester scans crop chlorophyll content (in correlation with N

content in leaves) based on different reflectance of red (653 nm) and infrared (931 nm) radiation. Chlorophyll content is recalculated by N-tester for a given crop variety (cultivar) and displayed as N need in kg N/ha. The N-tester is usually employed for setting N doses for cereals in production fertilization (BBCH 30-31, start of stem elongation) and qualitative (late) fertilization (BBCH 39-49, end of stem elongation to start of heading), as for central European conditions. GreenSeeker monitors and records NDVI as canopy-reflected radiation in RED and near-infrared spectrum (NIR). NDVI is in a close correlation with crop biomass and chlorophyll. Fertilizer N dose is given by a reference value (from the densest crop cover) and expected yield.

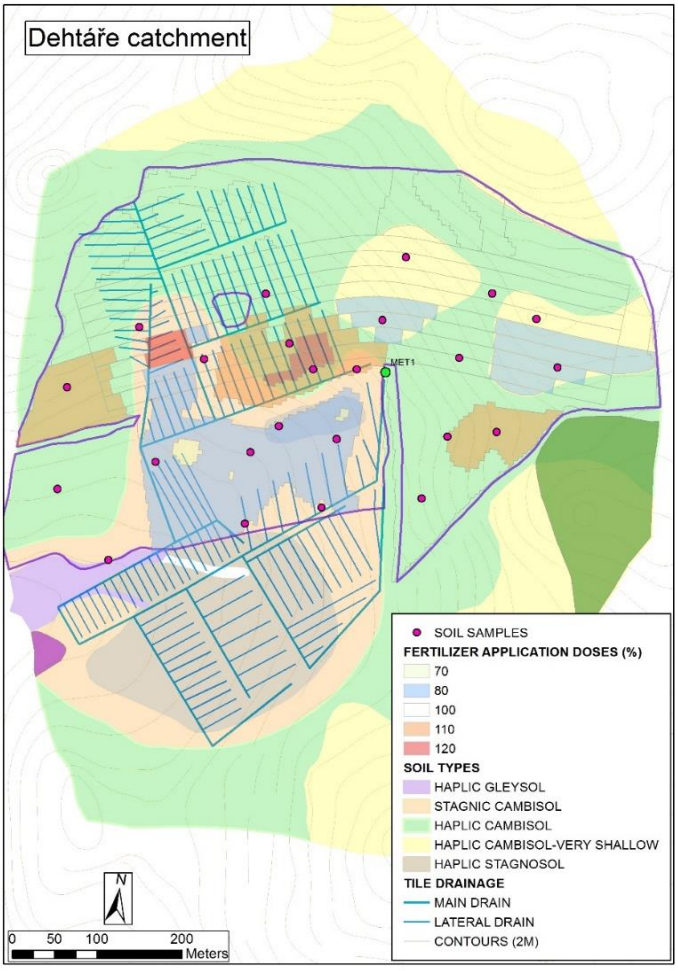

Figure 3-3. Variable fertilizer application zones for Dehtáře pilot site (2016)

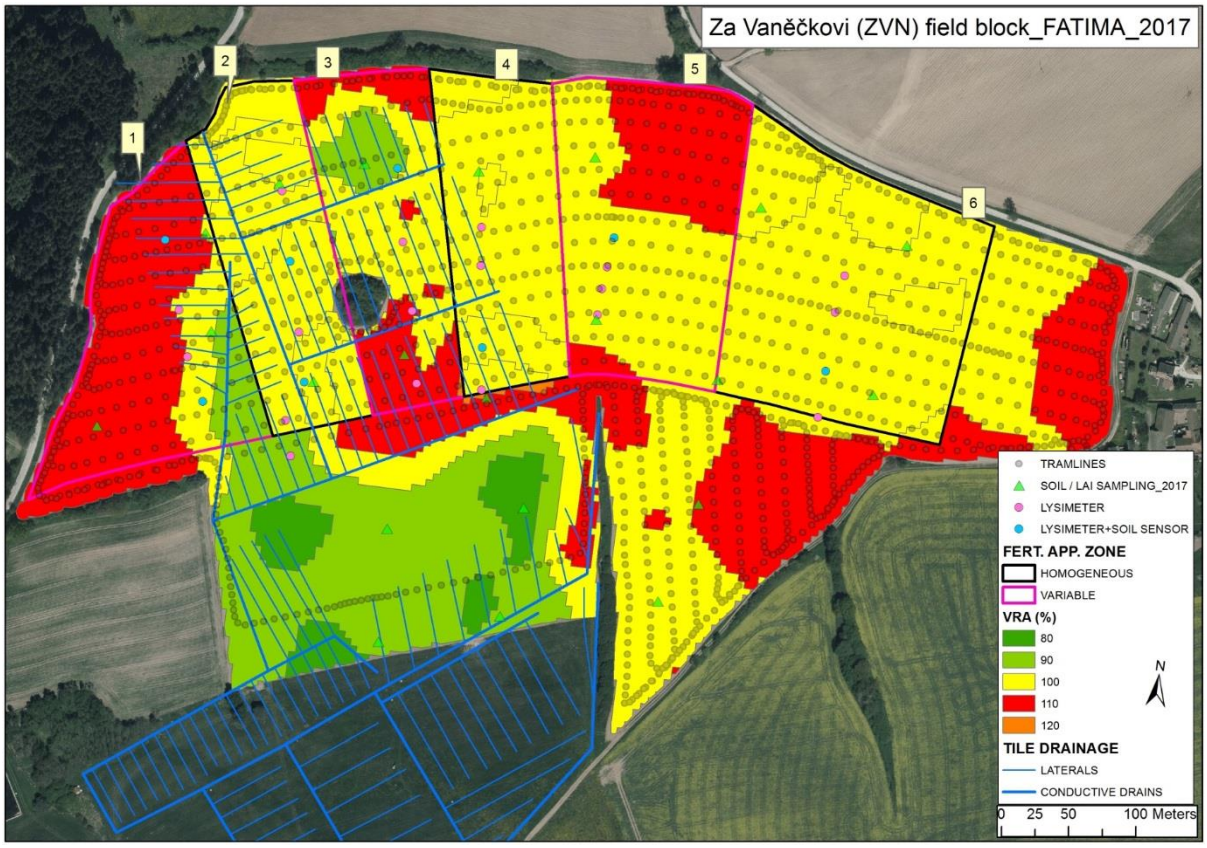

Figure 3-4. Variable fertilizer application zones for Dehtáře pilot site (2017)

Monitoring of crop spectral characteristics by the aforementioned hand devices took place between May - July, in a fortnight interval, on around 20 sites within the pilot field trial polygon. Results of N-tester (usually for the third – the last - fertilizer application) were incorporated in adjustment of late N fertilization and applied on the same or the next day. Recommended values for N doses from N-tester were averaged and this value was applied in the reference application zones (100% yield potential). In the other application zones, the applied N dose was set according the appropriate zone (e.g. 80% = 0.8 x 28 kg N/ha, etc.).

Satellite images from Sentinel 2A/B were not used due to dense clouds in the area and with only several cloudless images in the whole vegetation season (2016: 3; 2017: 7).

3.1.6 Yield potential method (3)

The approach was qualitative evaluated by demonstrating it in real-time applications with two farmers in winter wheat in 2017. A comparison between our yield potential map and the biomass map generated by the Yara N-Sensor was also done.

3.1.7 Crop model approach

3.1.7.1 Field experiment

The experimental site, situated in south of France consisted of a 6 hectares field which was established with durum wheat for two consecutive years (cv. Babylone in 2014-2015, cv. Pastadou in 2015-2016). Fertilizer application was split in three applications during the 2015-2016 growing season. The whole field received 44 kg N ha^{-1} as 22:16:0 fertilizer in mid-January 2016, while the VRT experiment was run on the 2nd and 3rd application.

In accordance with the 2014-2015 yield map obtained from the farmer, five observation plots were set-up, at the beginning of the 2015-2016 growing season, to mirror part of the high variability observed with yields (Figure 2.16). Soil sampling was carried out at each plot throughout the 2015-2016 growing season. Soil samples were subsequently analyzed for gravimetric water and mineral N content. Crop development (LAI, biomass, yield) was also monitored at each plot.

In the area, it is common practice to first apply mineral N fertilizer on wheat during winter, at the three leaves stage. Another two applications usually occur in spring, both at the end of the tillering and the stem elongation stages. The N application rate for the 2nd and 3rd application is usually calculated from an averaged field N balance method, taking into account the crop N requirements and the N supply from the soil. In order to compare such field N balance method with the VRT approach, the field was divided into two areas (Figure 3.5). A small area (=82 cells in the field grid) was fertilized using a variable rate application method, while the rest of the field was fertilized according to the results of an averaged field N balance. Three plots (E3050, E30, and E) were included in the modulated area, while the VRT approach was not used on the O30 and O plots.

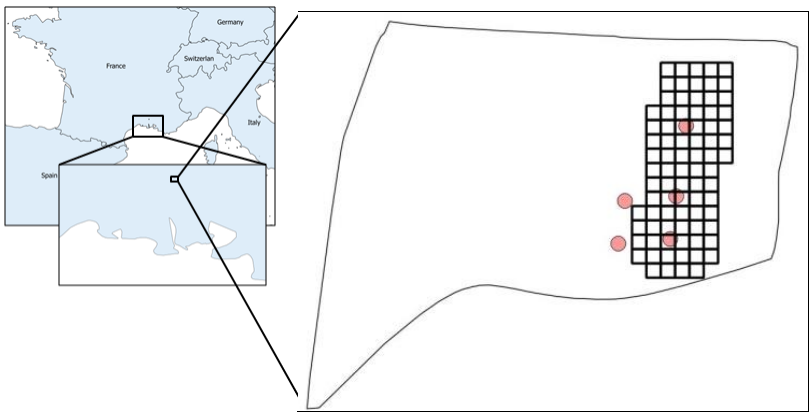

Figure 3-5. Geographical location of the Tarascon field. Experimental plots are shown in red circles while the black grid represent the area where the VRT approach was applied.

3.1.7.2 Estimation of soil water storage capacity from 2014-2015 observations

A sequential analysis of six multispectral SPOT 5 satellite images, collected in spring 2015, was carried on to estimate the LAI dynamics during the growing season. A spatialized grid (10x10m) was built from the pixel definition of SPOT 5 images and was used to re-shape the 2015 yield map provided by the farmer so that all the information could be displayed within the obtained grid. Pixels were classified in 7 homogeneous groups (accounting for more than 75% field variability) whose main source of variability was assumed to be soil water storage capacity (Figure 2.15).

As proposed by Varella et al. (2010), an inversion procedure (see paragraph 2.7.1.1.) was then carried on for each group to estimate both the soil water content at field capacity (for each soil layer) and the thickness of the deeper soil layer. For this case study, plant parameters of a medium-length cycle variety (cv. Lloyd) were used (rather than a newly calibrated STICS variety), as such variety was identified as the most similar STICS default variety to the actual one in place (cv. Babylone).

3.1.7.3 In-season estimation of plant density using drone imagery

The spatial variability of LAI and chlorophyll content was assessed on February 18th, 2016, from an aerial unmanned drone flight. LAI and chlorophyll content were estimated by inversion with the PROSAIL model with no prior information (Verger et al., 2014). LAI and chlorophyll estimations were then re-calibrated for the pixels containing the five observation-plots set-up in the field. Field LAI and chlorophyll estimations were corrected according to linear regression equations obtained from the field observations.

The LAI information was used to invert the STICS model and retrieve spatially-distributed plant densities (Figure 2.16). Those densities were within the range of densities observed in the plots (220 to 340 plants m^{-2}). The inversion procedure was performed for each homogeneous group. Once again, plant parameters from of a medium-length cycle variety (cv. Lloyd) were used as such variety was identified as the most similar STICS default variety to the actual one in place (cv. Pastadou).

3.1.7.4 Calculation of the fertilizer N recommendation

In this study, the crop requirement for a well-developed wheat crop was estimated to be 3.5 units of N intake to produce 100 kg of grain with 13-14% protein content. The average field N balance calculation also takes into account the initial soil mineral N content (to 1 m soil depth) and an estimate of 30 kg N ha-1 provided by the mineralization of the soil organic matter and crop residue. Such reference method was applied in most parts of the field, including two monitored field plots (O and O30).

At the 2nd and 3rd fertilizer applications, the VRT approach was applied on the 82 cells area selected in the field (paragraph 3.1.7.1. and Figure 3.5), including three monitored plots (E, E30 and E3050). Fertilizer N application rates were calculated according to the method presented in the paragraph 2.7.1.3.

3.2 Benchmarking

3.2.1 Methodology

The simulator is based on a computer environment permitting a multisimulation of the STICS crop model. Each simulation corresponds to a pixel of 10mx10m corresponding to the pixel of the satellite S2A. The simulator uses

- a varietal parameterization calibrated for the crop in question,
- a soil map addressing the main sources of variability
- an assessment of the quality of of the crop explaining installation explaining the variability of the LAI before the decision making for fertilization (15/02)
- climatic conditions of the considered year.
- N application dose applied on every pixels provided by the different methods

For every fertilization recommendation we applied the same fertilization calendar by only changing the fertilization dose. In the case of the simulator carried out on the Tarascon plot in 2016, the different stages were carried out in the following way:

- The Lloyd wheat variety parameterization was taken as closest variety to that cultivated in 2016 (PASTADOU). The selection of the variety was made by considering both the LAI dynamic and the yield.

- The considered soil properties are the volumetric water content at the wilting point and that at field capacity. These were obtained using an inversion procedure as described in part 2.6.1
- The quality of the crop implantation was made by adjusting the sowing depth leading to the LAI observed with a drone made by February 17th (Fig 3.6) show clearly a strong heterogeneity at the beginning of the crop). The sowing depth is an efficient way to delay emergence date as well as emergence rate. This is a typical pattern of crop emergence since late emergence is often linked to seedling mortality.

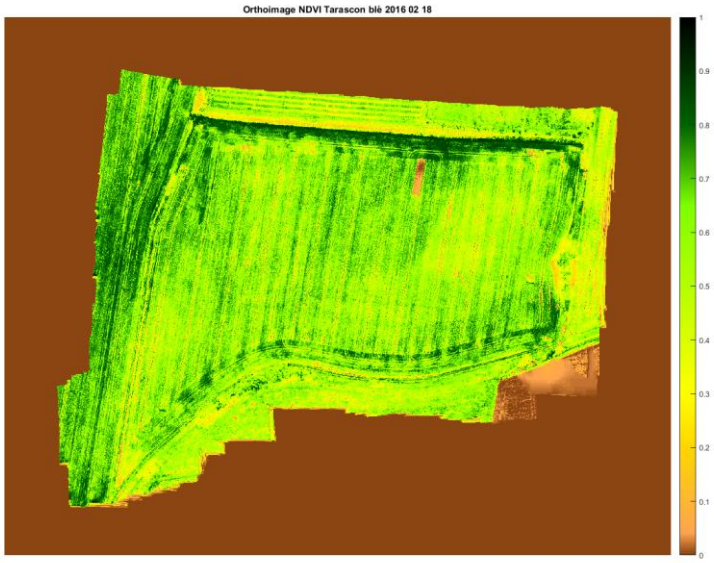

Figure 3-6. NDVI map of Tarascon Field from a Drone the February 18th 2016

- Soil water content initialization was done by considering a soil at field capacity after heavy rainfalls and soil initial nitrogen was assumed to be homogeneous at the average value measured in the field.
- Climatic data from the Tarascon were used for the simulations.

3.2.2 Evaluation of the STICS model to represent Yield sensitivity to Nitrogen fertilization

The Nitrogen Trial made on Dehesa fields by UCLM partner was used to test the the ability of the Stics model to represent the Yield response to Nitrogen fertilisation dose. A sensitivity of the yield of every Dehesa plot to the nitrogen application simulated by the STICS model is shown in Figure 3.7. Results have shown a strong sensitivity of the STICS model to the nitrogen dose, which is consistant with the ability of the measurements. This give some confidence for using the STICS model as a fertilisation recommandation simulator.

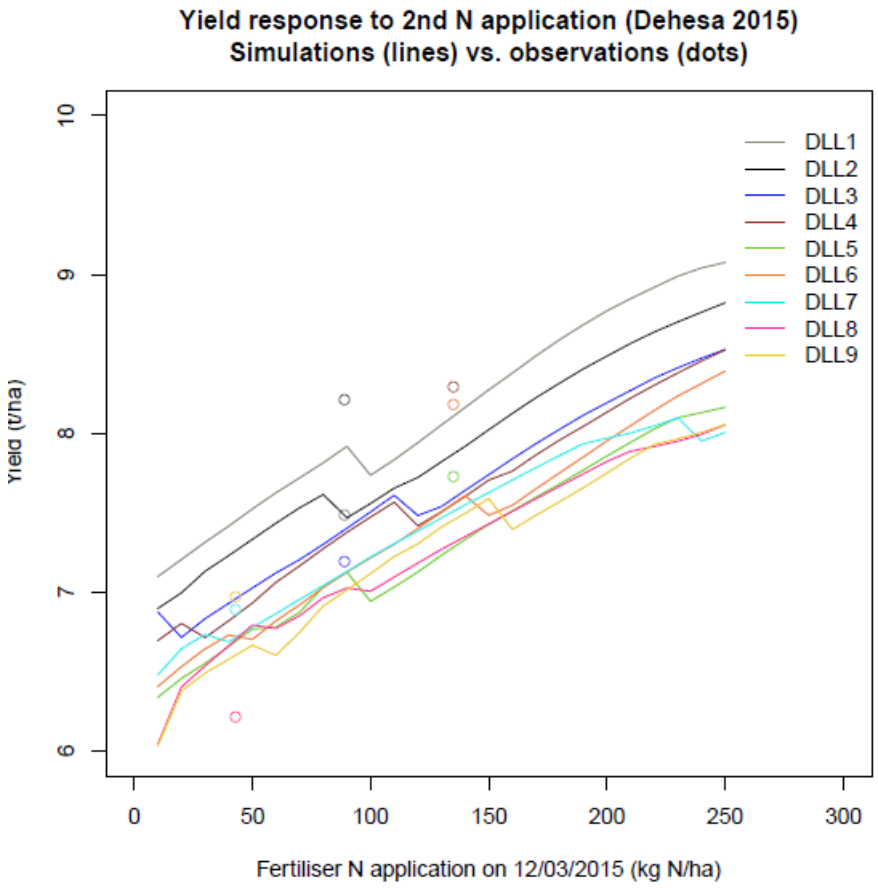

Figure 3-7. sensitivity analysis of the STICS models to Nitrogen application dose (2nd fertilization). Lines correspond to the simulations, Points corresponds to measurements.

3.2.3 Sites descriptions

3.2.3.1 Tarascon field (France)

Site Feature	**Map** of the site showing the heterogeneity in the previous year (2014-2015)
Crop: Durum wheat (cv. Pastadou) Spatial information: - Remote-sensing acquisitions: 13 dates from 05/02/2016 to 27/06/2016 (S2A) - Yield map: yes (02/07/2016) Crop management: - Residue management: wheat residues ploughed in before sowing - Sowing date: 17/11/2015 - Sowing density: 280 seeds m^{-2} - Irrigation: No - Fertilization: 44 kg N ha^{-1} on 14/01/2016, 50 to 90 kg N ha^{-1} on 04/03/2016, 60 to 100 kg N ha^{-1} on 08/04/2016	- Soil WSC map 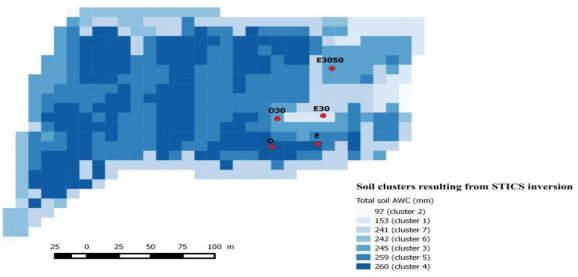 - Yield map at harvest on 02/07/2016

Field area: 6 ha

Soil type: Calcaric-fluvisol (FAO classification, 1974)

Main sources of heterogeneity:

- Soil texture
- Soil initial mineral N content

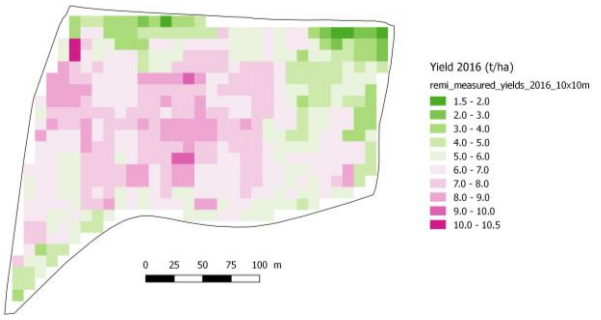

How heterogeneities are accounted for in crop models:

Soil map: Spatial distribution of soil water storage capacity can be taken into account through the estimation, for each simulation unit (= 1 grid cell on the maps), of the soil moisture at field capacity and wilting point, as well as the soil depth. Model inversion procedures are used for such estimations.

Crop development: The quality of crop establishment can be accounted for through the estimation, for each pixel, of model-based sowing densities and depths, in order to mirror the crop emergence density and / or early season LAI observed in the field.

Nitrogen initialization: Spatial distribution of initial soil NO_3-N content, at the start of the simulation, can either be estimated from extensive field measurements or inverted from LAI observations until flowering

STICS implementation :

The STICS model was parameterized as follows:

- Weather data recorded at meteorological station nearby were used for the simulation.
- Plant parameters were taken from an existing STICS default variety (cv. Lloyd) as such variety was identified as quite similar to the actual one in place (cv. Pastadou).
- Crop management information (soil tilling, crop residues management, fertilization…) was provided by the farmer. However, sowing density was corrected by inversion on the early-season LAI data.
- The STICS soil component was parameterized from field measurements in the most representative soil clusters (O and E sampling points), and only the soil WSC was estimated by inversion.

Field heterogeneity was addressed here using the spatial distribution of inverted soil WSC, sowing density and initial soil NO_3-N content.

STICS Results

Show the ability of the model to reproduce vegetation dynamic, yield and nitrogen release

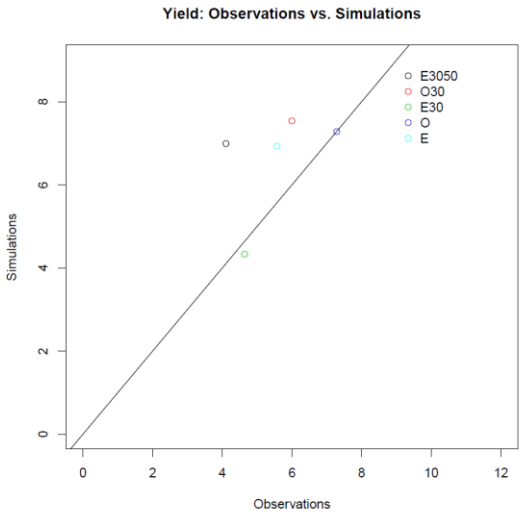

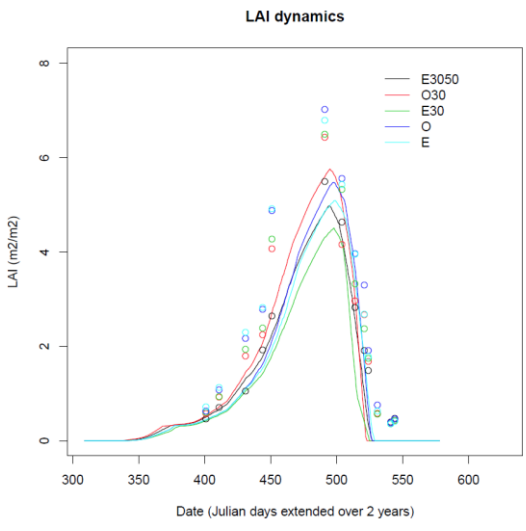

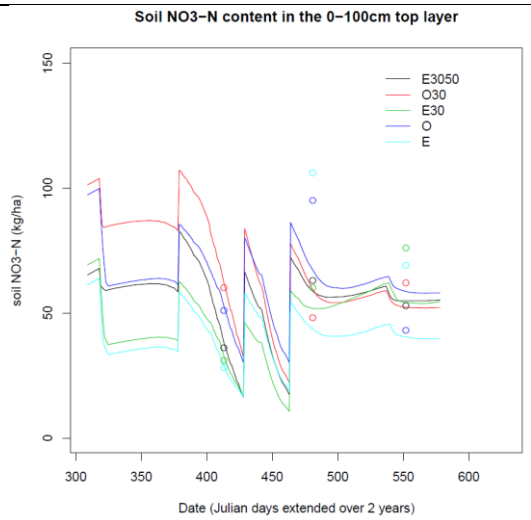

3.2.3.2 Avignon field (France)

Site Feature

Crop: Durum wheat (cv. Isildur)

Spatial information:

- Remote-sensing acquisitions: 10 dates from 03/01 to 02/06/2017 (S2A)
- Yield map: no

Crop management:

- Residue management: wheat residues ploughed in before sowing
- Sowing date: 16/11/2016
- Sowing density: 350 seeds m^{-2}
- Irrigation: No
- Fertilization: 36 kg N ha^{-1} on 11/01/2017, 102 kg N ha^{-1} on 08/03/2017, 70 to 150 kg N ha^{-1} on 12/04/2017

Field area: 2 ha

Soil type: Calcic-cambisol (FAO classification, 1974)

Main sources of heterogeneity:

- Soil depth
- Soil initial mineral N content
- Crop establishment

Map of the site showing the heterogeneity

- Resistivity map (related to soil depth)

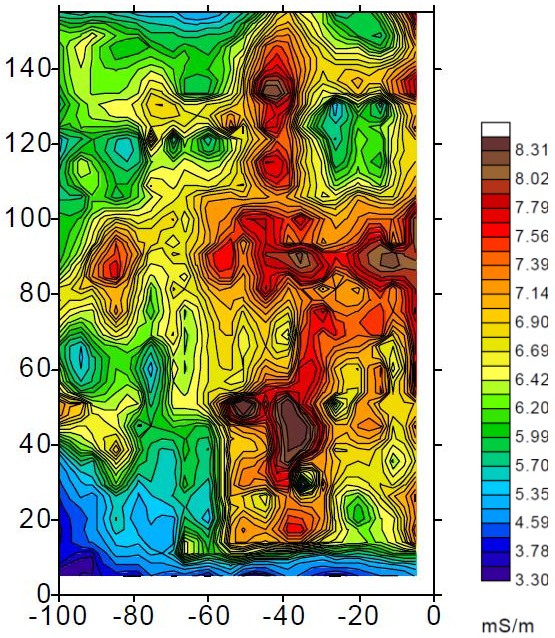

How heterogeneities are accounted for in crop models:

Soil map: Spatial distribution of soil water storage capacity can be taken into account through the estimation, for each simulation unit (= 1 grid cell on the maps), of the soil moisture at field capacity and wilting point, as well as the soil depth. Model inversion procedures are used for such estimations.

Crop development: The quality of crop establishment can be accounted for through the estimation, for each pixel, of model-based sowing densities and depths, in order to mirror the crop emergence density and / or

early season LAI observed in the field.

Nitrogen initialization: Spatial distribution of initial soil NO_3-N content, at the start of the simulation, can either be estimated from extensive field measurements or inverted from LAI observations until flowering

STICS implementation :

- Weather data recorded at meteorological station nearby were used for the simulation.
- A new durum wheat variety was calibrated for the STICS model to better reproduce field observations.
- Crop management information (soil tilling, crop residues management, fertilization…) was provided by farm managers. However, sowing densities and depths were corrected by inversion on the early-season LAI data.
- The STICS soil component was parameterized from field measurements in the most representative soil, and only the soil WSC was estimated by inversion.

Field heterogeneity was addressed here using the spatial distribution of inverted soil WSC, sowing density and initial soil NO_3-N content.

STICS RESULTS

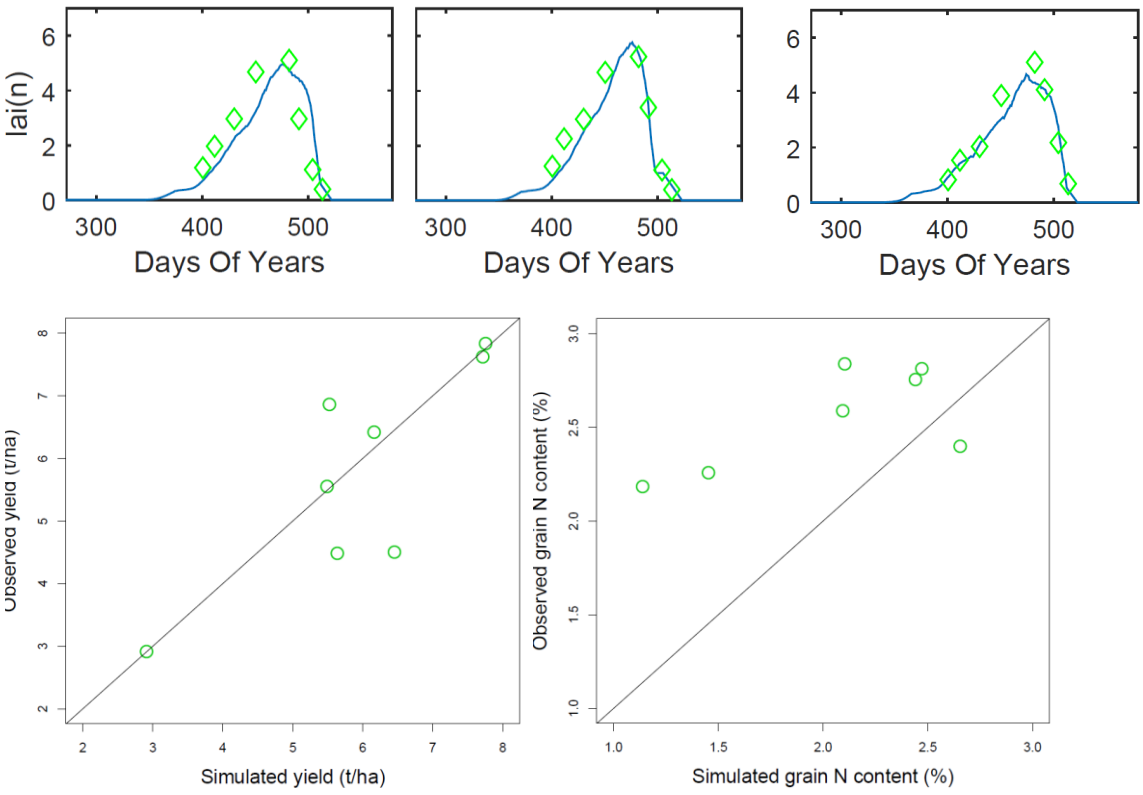

3.2.3.3 Dehesa field (Spain)

Site Feature	**Map** of the site showing the heterogeneity
Crop: Bread wheat (cv. Califa) Spatial information: - Remote-sensing acquisitions: 6 dates from 10/03 to 23/06/2015 (L8) - Yield map: yes (10/07/2015) Crop management:	- Productivity map (UCLM, 2015)

- Residue management: maize residues ploughed in before sowing
- Sowing date: 17/01/2015
- Sowing density: 820 seeds m^{-2}
- Irrigation: 444 mm (split in 41 irrigation events from 28/02 to 20/06/2015)
- Fertilization: 60 kg N ha^{-1} on 31/12/2014, 43 to 135 kg N ha^{-1} on 12/03/2015, 3 x 30 kg N ha^{-1} fertigation on 18/04/2015, 28/05/2015 and 06/06/2015 respectively

Field area: 42.6 ha

Soil type: Calcic-cambisol (FAO classification, 1974)

Main sources of heterogeneity:

- Soil depth
- Soil organic matter content

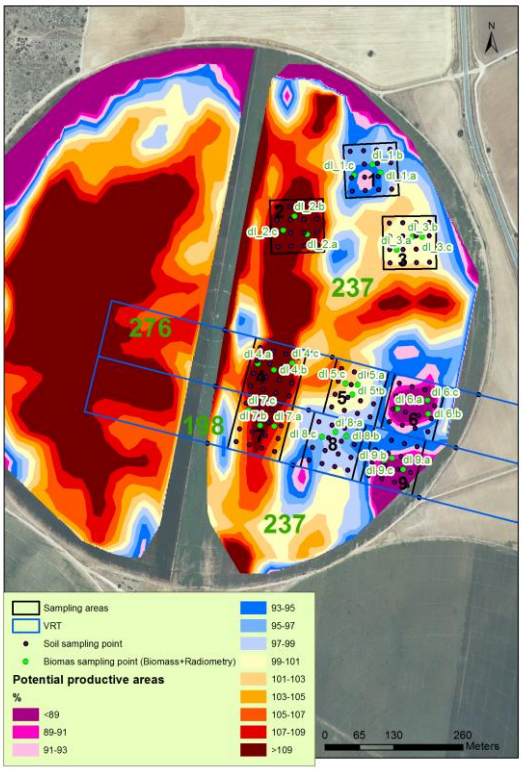

How heterogeneities are accounted for in crop models:

Soil map: Spatial distribution of soil water storage capacity and organic matter content can be taken into account through the estimation, for each simulation unit (= 1 grid cell on the maps), of the soil organic N content and depth. Model inversion procedures are used for such estimations.

Crop development: The quality of crop establishment can be accounted for through the estimation, for each pixel, of model-based sowing densities and depths, in order to mirror the crop emergence density and / or early season LAI observed in the field.

Nitrogen initialization: Spatial distribution of initial soil NO_3-N content, at the start of the simulation, can either be estimated from extensive field measurements or inverted from LAI observations until flowering

STICS implementation :

describe the method for the crop model parameterization and how the spatial variability is addressed

- Weather data recorded at meteorological station nearby were used for the simulation.
- A new bread wheat variety was calibrated for the STICS model to better reproduce field observations.
- Crop management information (soil tilling, fertilization…) was provided by farm managers. However, sowing densities and depths were corrected by inversion on the early-season LAI data.
- The STICS soil component was parameterized from field measurements in the most representative soil, and only the soil organic N content and depths were estimated by inversion.

Field heterogeneity was addressed here using the spatial distribution of inverted soil organic N content, soil depth, crop emergence density and initial soil NO_3-N content.

STICS Results

Show the ability of the model to reproduce vegetation dynamic, yield and nitrogen release

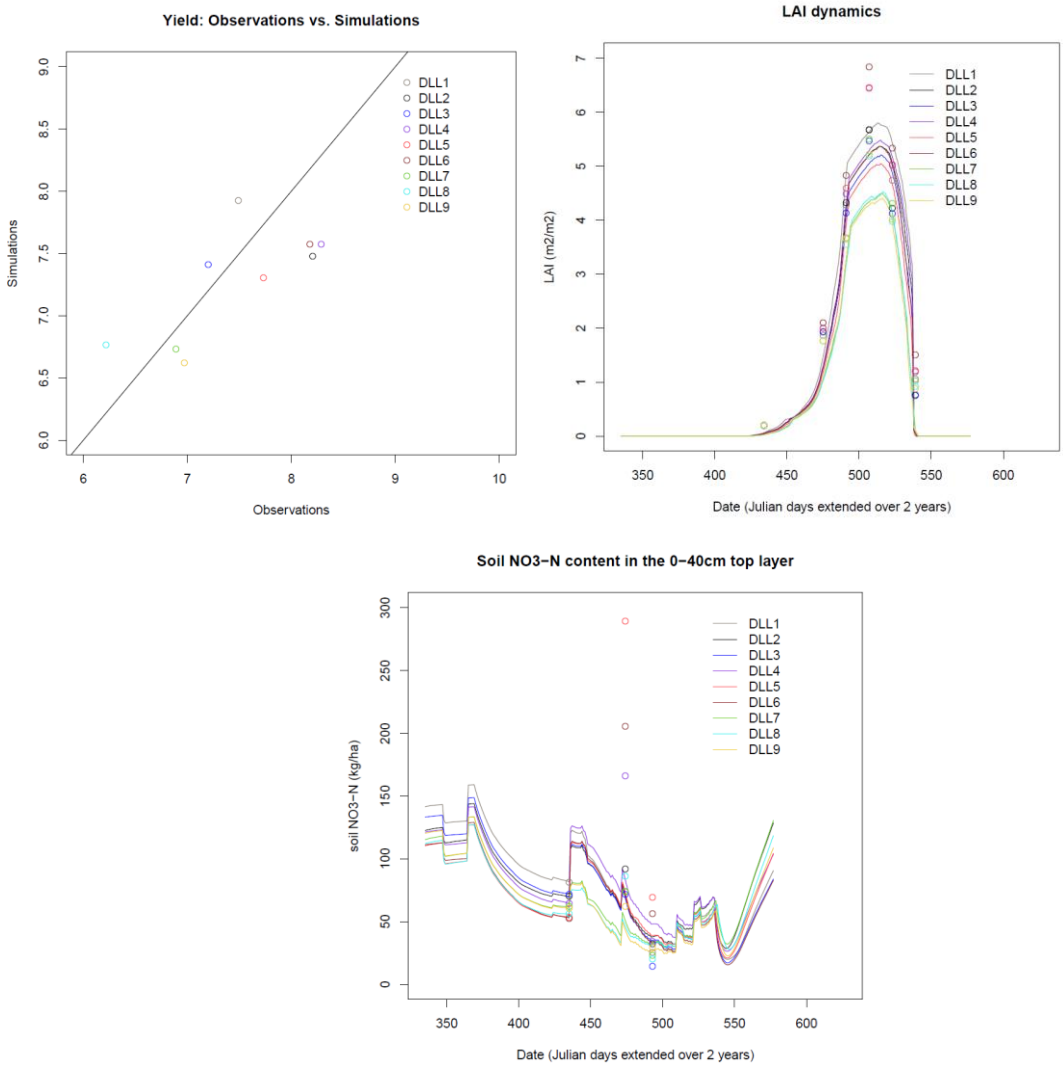

3.2.3.4 Tarquina field measurements

Site Feature

Crop: Durum wheat

Spatial information:

- Remote-sensing (S2A) acquisitions: 9 in 2016 (17/01 to 25/06) and 8 dates in 2017 from (15/03- 23/06)
- Yield map: no

Crop management (2016):

- Residue management: deep ploughing, spike tooth harrow, tandem disc (20/10-6-11)
- Sowing date: 26/12/2015
- Sowing density: 400 seeds m^{-2}
- Irrigation: No
- Fertilization: Mineral 40 NP 26/12/2015, 52 NH4-NO3 2/03/2016, 39 NH4-NO3 31/03/2017
- Harvest : 2/07/2016

Map of the site showing the heterogeneity

- Topographic maps

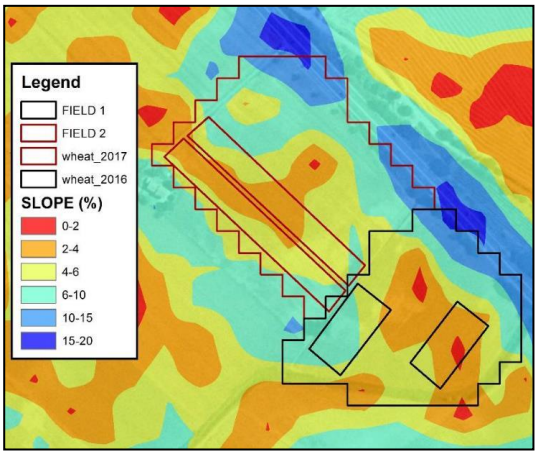

Lai maps

Field area: 5 ha

Soil type: Soils: (VRD1) Haplic Phaeozems - fine-loamy mixed thermic; (SGU1) Haplic Cambisols – fine loamy mixed thermic, according to IUSS-WRB, 2015.

Main sources of heterogeneity:

- Soil organic matter
- Topography

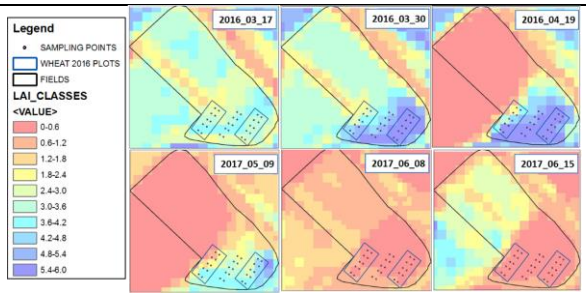

Soil organic matter

Year	2016	2017
	TOPSOIL	
MIN	0.574	0.434
MAX	0.877	1.058
MEAN	0.740	0.645
SD.DEV.	0.092	0.200
	SUBSOIL	
MIN	0.438	0.439
MAX	0.442	0.443
MEAN	0.441	0.441
SD.DEV.	0.001	0.001

4 Results

4.1 Field test

When available we can show fertilization map and their impact on yields, conclusion on the efficiency)

4.1.1 SI approach (Greece – Larissa))

Based on the results of the field strip experiments to date, a general comparison of VRA and farmer practices is presented in terms of environmental and economic criteria. In essence, the comparisons refer to four field experiments in three different crops. A fifth cotton experiment is still in progress while the wheat experiment performed during the 2016-17 growing season was constrained due to lack of crop response to fertilizer applications as a result of adverse weather conditions. The developed high-resolution system used to apply VRA in field strips and an in-depth analysis of plot data that compares the spatial performance of VRA to other treatments is reported in other deliverables.

The strip yields attained by the VRA system were comparable to those of the farmer practice with differences ranging from -3 to +1% (Table 4.1). Only in one instance VRA yield was considerably higher than the farmer practice (12% higher in the cotton 2015 trial). The relatively higher crop N values in the farmer strips were caused by higher grain N uptake as a result of increased N inputs.

Table 4-1. Comparison of VRA to farmer strip yields in the Greek pilots

Crop	Year	Crop yield (kg/ha)		Change (%)	Grain N (kg N/ha)		Change (%)
		VRA	Farmer	VRA/Farmer-1	VRA	Farmer	VRA/Farmer-1
Wheat	2016	5891	5815	0.01	134	152	-0.12
Wheat	2017‡	4082	4200	-0.03	96	91	0.06
Cotton	2015	3465	3087	0.12	69†	61†	0.13
Cotton	2016	2885	2988	-0.03	57†	59†	-0.03
Cotton	2017	in progress			in progress		
Corn	2017	13365	13796	-0.03	130	135	-0.04

† Estimated seed N was based on data from Stamatiadis et al. (2016)

‡ The wheat 2017 experiment was constrained due to lack of yield response to fertilizer N

The advantage of VRA over farmer practice was the significant reduction of N inputs ranging from 24 to 42% (Table 4.2). The reduction of applied N over comparable yields resulted in agronomic NUEs 13 to 31% higher than those of the farmer practice (Table 4.2). These increases in NUE translate to equivalent reduction of N losses due to leaching, denitrification, immobilization and ammonia volatilization. It is noted that the optimal in-season N rate (N_{opt} in equations 2 and 3) was the conceived optimal rate used by the farmer and tends to be in excess of the rate that would otherwise be used by mass balance. However, this is a realistic approach as the mass balance parameters are unknown entities in most agricultural fields. It should also be noted that the percent reduction of N_{opt} by VRA is field- and growth stage-specific and is independent of the absolute amount applied by the farmer.

Table 4-2. Comparison of VRA to farmer N-use efficiencies in the Greek pilots

Crop	Year	Grain N (kg N/ha)		Total N applied (kg N/ha)		% Change	NUE (%)	
		VRA	Farmer	VRA	Farmer		VRA	Farmer
Wheat	2016	134	152	131	212	-0.38	103	72
Wheat	2017‡	96	91	146	150	-0.03	66	60
Cotton	2015	69	61	126	214	-0.41	55	29
Cotton	2016	57	59	94	162	-0.42	61	36
Cotton	2017	in progress		134	200	-0.33	in progress	
Corn	2017	130	135	205	270	-0.24	63	50

‡ The wheat 2017 experiment was constrained due to lack of yield response to fertilizer N

4.1.2 NNI approach- 1

The values of NNI have evidenced a variability within the field which has been reflected in the final biomass production. In the map of NNI below (Figure 4.1), referred to 15th March 2017, in correspondence of the red-dots, we notice that the value of NNI is slightly higher in correspondence of points 1-2 and 10, which were also corresponding to the highest values of final biomass. This difference is more evident in the map

of Figure 4.2, corresponding to 21st April 2017, where we observe lower values of NNI (yellow colors) in correspondence of the central part of the experimental field with lower final biomass.

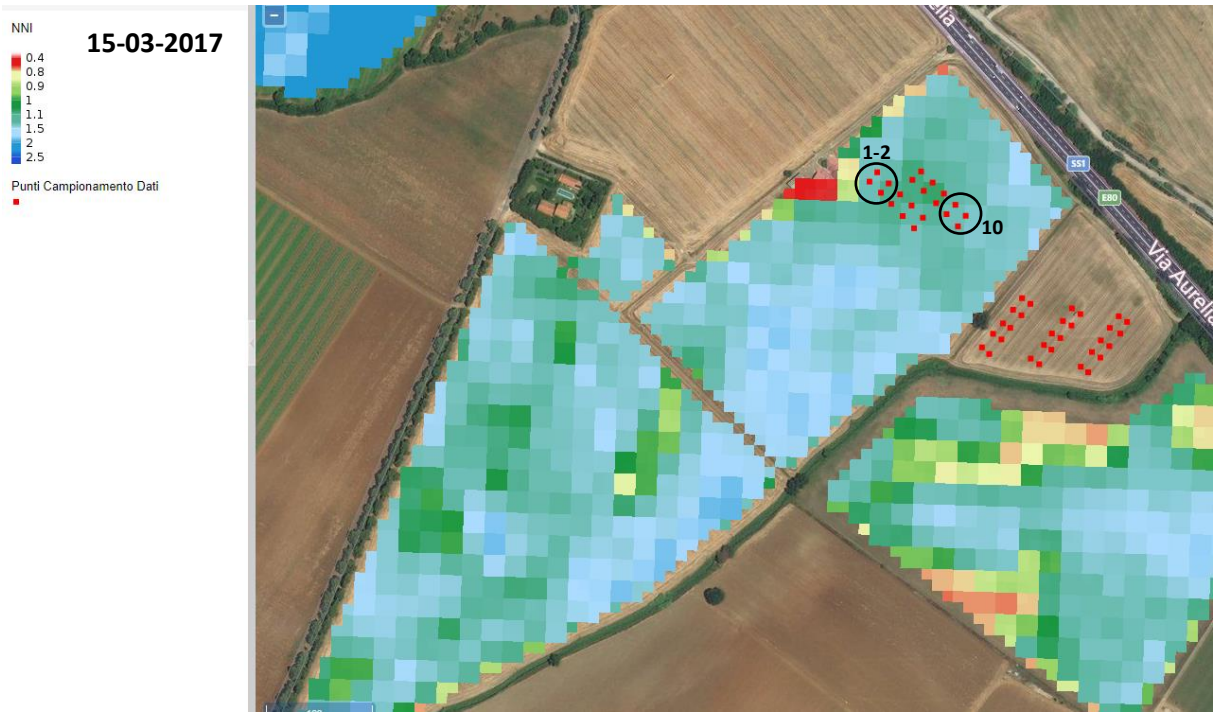

Figure 4-1. Map of NNI – durum wheat 15th March 2017, Tarquinia (I) test site.

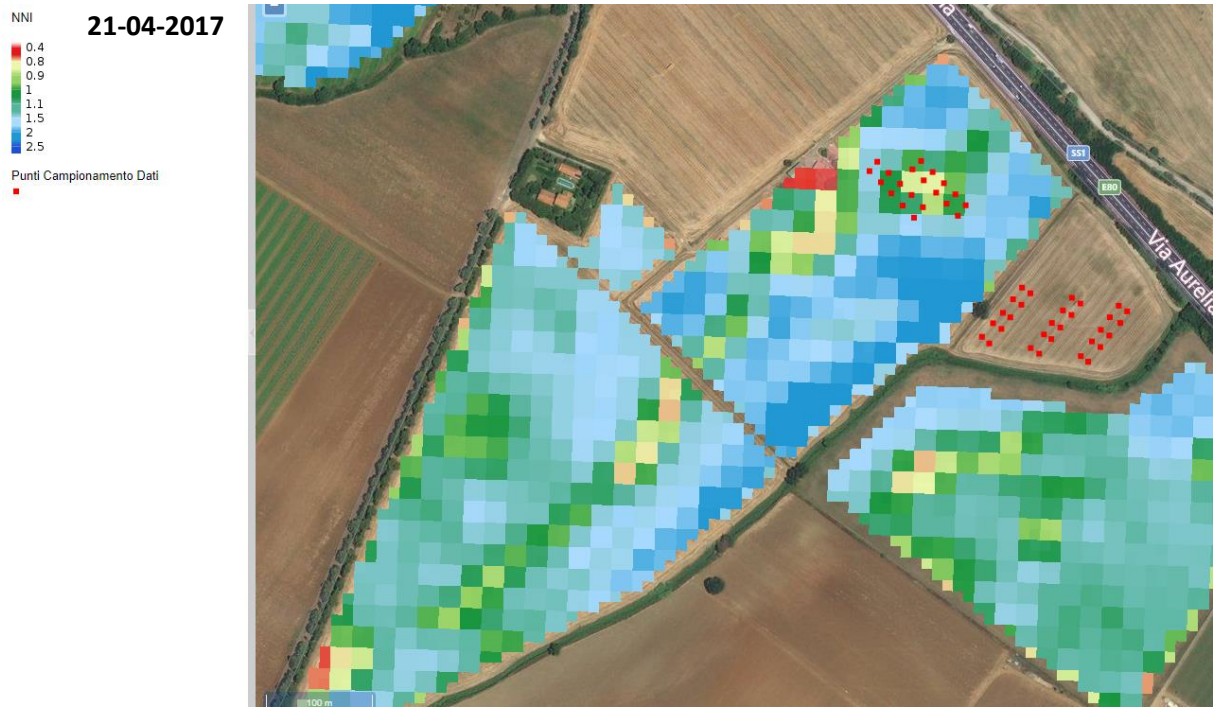

Figure 4-2. Map of NNI – durum wheat 21st April 2017, Tarquinia (I) test site.

Other experimental data acquired over the test site of Tarquinia evidence that the maps of NNI reproduce the observed spatial pattern of final yield. In this specific case, no VRT was available, so it was not possible to compensate for the variability of NNI already observed in March. However, the maps of NNI have proved

to be an useful indicator of the spatial variability of the nutritional status of wheat. This implementation of NNI has been based on the calibration carried out during the field campaign of 2016. From the validation made by using field data acquired in 2017 it is possible to conclude that the calibration was still valid, for the same wheat variety in the Tarquinia site. Further research is needed – possibly with similar datasets – to derive a crop-specific calibration for NNI from Sentinel-2 red edge indexes.

4.1.3 NNI approach -2

The measured $\%N_a$ and dry mass for the 12 experimental plots (3 replicates with 4 N rates; N0: 0 kg N; N1: 60; N2: 120; N3: 180) were plotted for 2016 and 2017. The position of the points in respect to the experimental Nitrogen Dilution Curve indicates that all parcels were in N deficit. The temporal evolution of the Nitrogen Dilution of the 12 experimental plots is consistent with the experimental Nitrogen Dilution Curve (Figure 4.3).

The empirical functions to derive dry weight and %N from Sentinel-2 (S-2) data are shown in Figure 4.4. Amongst several indices, DCNI was the one that provided some correlation (R^2 = 0.46) with %N. For dry weight, the correlation with single-date S-2 LAI (closest to the ground-measure) was very good (R^2 = 0.84) and can certainly be improved by using seasonally cumulated LAI values.

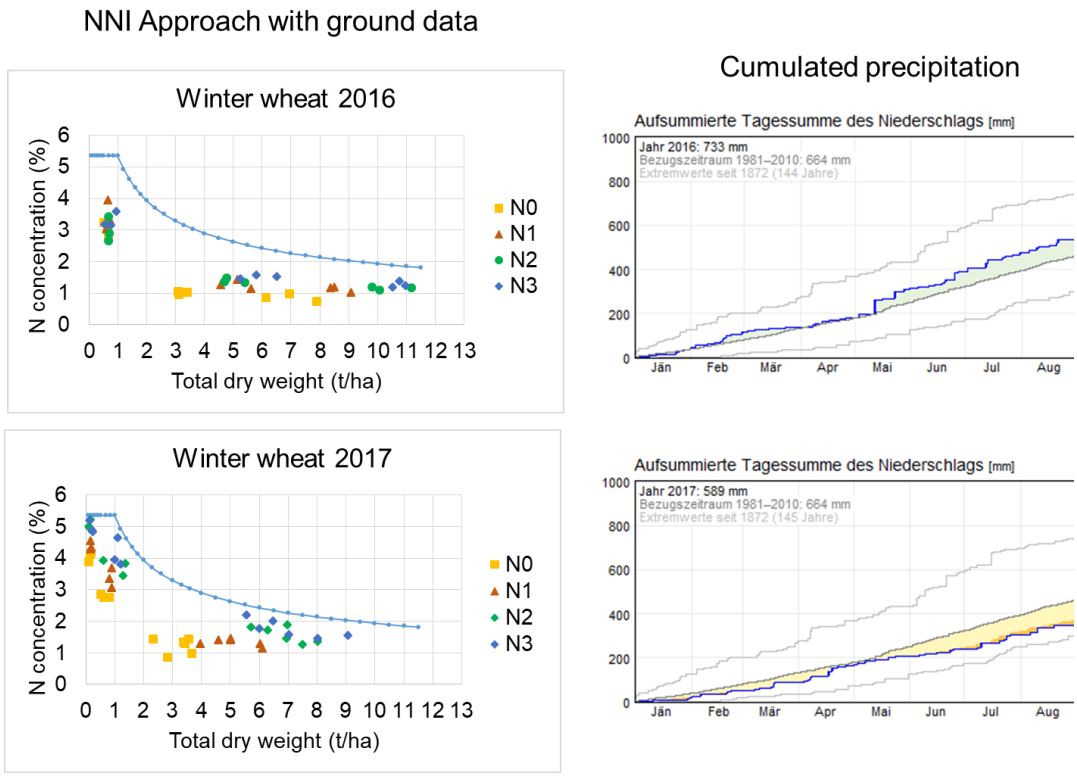

Figure 4-3. NNI approach with ground-based measurements for 2016 (wet year, max yield ~ 11 t/h) and for 2017 (dry year, max yield ~ 9 t/ha) (N0: 0 kg N; N1: 60; N2: 120; N3: 180).

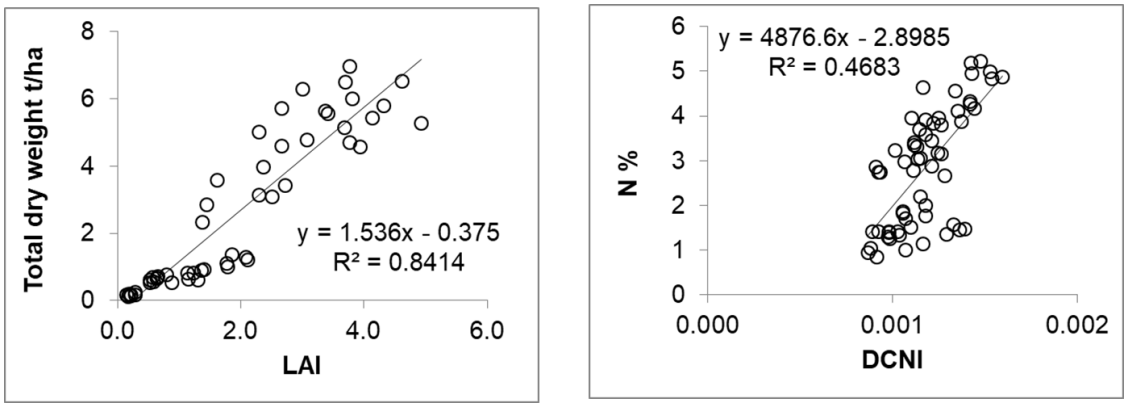

Figure 4-4. Empirical calibration to derive total dry weight (left) and %N (right) from Sentinel-2 data using LAI and DCNI, respectively. The scatterplots the 12 experimental plots for two years and 2 measurements campaigns in 2016 and 3 campaigns in 2017. The closest in time Sentinel-2 observation was used.

The LAI-W and %N-DCNI relationships were applied to the Sentinel-2 acquisition of and one exemplary result is presented in Figure 4.5.

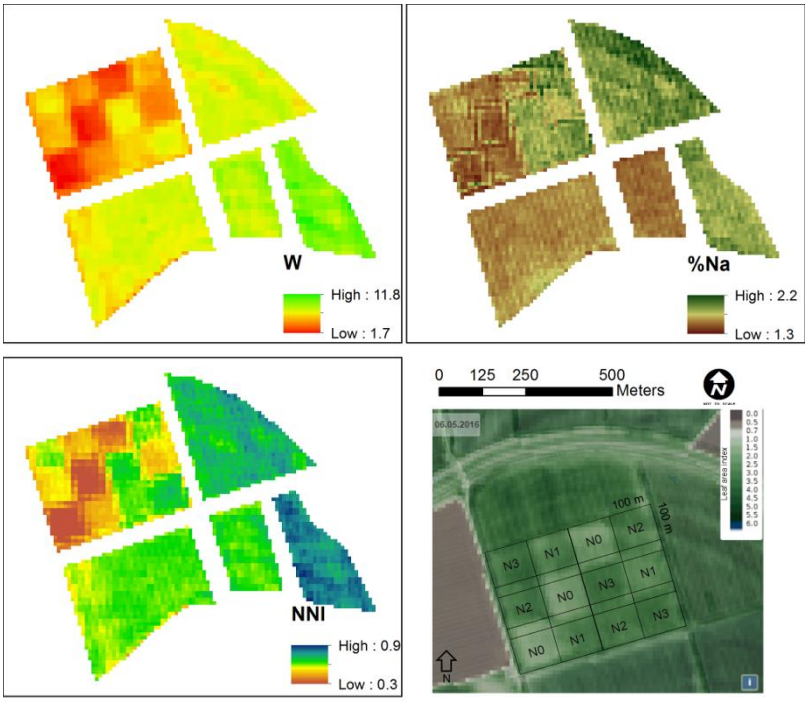

Figure 4-5. An example of mapping of the Total Dry Weight (top left), %N (top right) and derived NNI (bottom left).

4.1.4 Results of the EO-based yield potential method for the pre-season N recommendation.

4.1.4.1 Biomass production based on the temporal series of multispectral EO images

The results obtained for the calibration dataset revealed the capacity of the proposed approach to estimate biomass production for spring wheat in the study area. The values of LUE and WUE obtained for the analyzed datasets (1.77±0.02 $g \cdot MJ^{-1}$ and 4.40±0.05 $g \cdot l^{-1}$, respectively) were in the range of previous analyses relating biomass and transpiration of radiation absorption based on other approaches (measurements). Nevertheless, it is fair to say that the methodology proposed and the values of LUE and WUE must be regarded as empirical values, potentially affected by local conditions, i.e. climate, and other stresses not considered in the analysis. Previous research indicates the factors affecting the empirical values of LUE and WUE are related with the crop management, mainly water or nitrogen deficits, and the meteorological conditions such as temperature stress and atmospheric demand. For these reasons, the relationships obtained in this work were applied to the validation dataset with the aim of providing an empirical validation and assuring the reproducibility, and representability of the proposed approaches. In addition, the characteristics of the validation datasets allowed to analyze the proposed approach under nitrogen deficit and in two very different climatic conditions (Semiarid Mediterranean and Continental Sub-humid climates). The results obtained confirm the suitability of the proposed model for the assessment of biomass production in wheat. For an extensive analysis of the results obtained and additional discussion of the aptitudes of the different models the reader is referred to Campos et al. (2018).

4.1.4.2 Maps of within-field variability of yield production

The comparison of the measured and modeled variability (Figure 4.6) confirmed the capability of the model to reproduce the spatial variability in every monitored field. In addition, the model was able to reproduce the absolute yield for fields with higher production (fields 1, 2, and 6) and trend to overestimate the yield in the field with lower production (field 4). The range of the variability based on the measured and modeled data was around a 60% of the mean values for the most heterogeneous fields (field 4). The variability estimated for the most homogeneous fields (fields 1, 2 and 6) was lower than the 40% of the mean values (see). The precision of the model was considered adequate, being the RMSE lower than 0.07 for the comparison between measured and modeled variability. However, the proposed approach did not reproduce some of the effects affecting the spatial distribution of the crop yield. The values of the standard deviation (SD) presented in the Table 4.3 indicated that the range of yield estimated by the model was, in general, slightly lower that the measurements based on the yield monitor. This effect was evident for the fields 1, 2 and 3 and could be appreciated in the correlations showed in the Table 4.3. For these fields, the model trended to overestimate the crop yield in the less productive areas and the model underestimated the actual yield in the more productive areas. The noted discrepancies had the corresponding effect in the comparison in terms of variability.

Table 4-3. Summary of the results in terms of measured and modeled yield (Yie.) and statistics comparing the measured and modeled values of yield and variability (Var.) for the areas effectively monitored, excluding borders and unproductive zones. SD: Standard deviation; RMSE: Root mean square error; d: improved index of agreement (Willmott et al., 2012).

	Yield monitor		Modeled values		RMSE		d	
Field ID	Yie. average (t/ha)	SD (t/ha)	Yie. average (t/ha)	SD (t/ha)	Yie. (t/ha)	Var.	Yie.	Var.
1	8.82	0.47	8.91	0.20	0.37	0.04	0.63	0.64
2	7.51	0.43	7.52	0.29	0.34	0.04	0.64	0.64
3	7.45	0.52	7.29	0.23	0.42	0.05	0.61	0.61
4	4.03	0.76	3.99	0.60	0.27	0.07	0.83	0.83

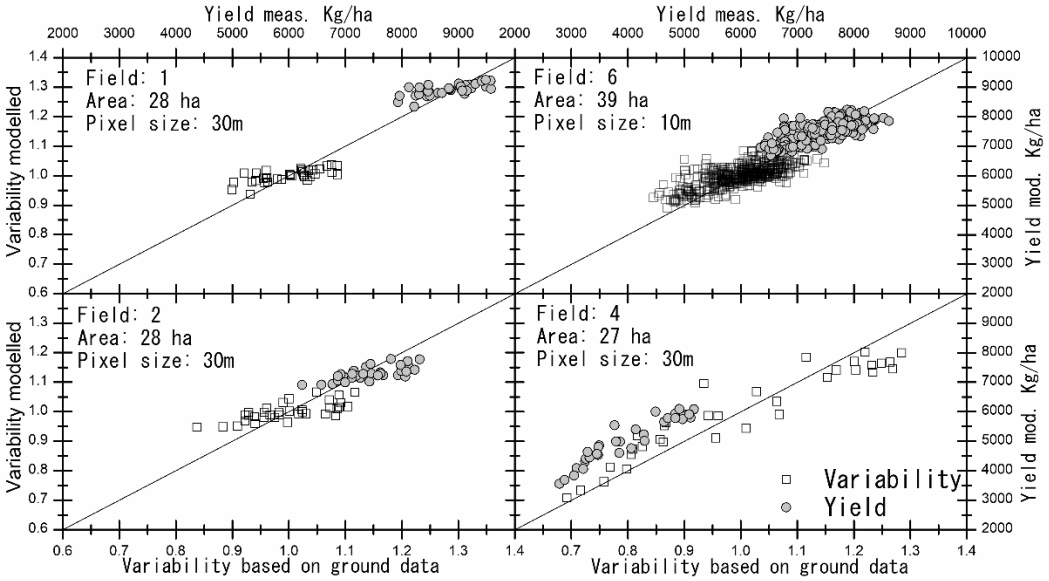

Figure 4-6. Comparison of measured and modelled yield and variability estimated based on the yield monitor and the approach proposed in the text. The areas indicated in the graphs correspond to the areas effectively monitored, excluding borders (1 pixel) and unproductive zones.

Attending to the parametrization of the model, the main sources of uncertainty for the simulation of the within-field variability are the possible effect of the stresses not considered in the proposed approach and the consideration of a fixed value of the harvest index. In addition to the possible effect of the various stresses increasing the variability at field scale, the assumption of a fixed value of HI could reduce the sensibility of the model to reproduce this variability. In consequence, an intensive research line is the development of simplified approaches that considers the whole spectrum of stresses affecting the spatial variability of yield/biomass production. In the areas monitored, the main stresses detected are water and nitrogen stress. The experience obtained, based on the empirical evaluation of the proposed approach with respect to grain and biomass production data, indicates that the model centered on biomass exhibits a trend on overestimating the actual values under water stress conditions. In addition, the variability reflected by the model is lower that the variability measured in the field. The Figure 4.7 shows the comparison of measured and modelled yield and biomass data in a rainfed field cultivated with wheat during the year 2016 (field 7). As indicated, the model trend to overestimate the experimental data in the areas with lower productivity and presumably subjected to higher stress conditions.

The approaches under development try to calibrate the spatial distribution of the stresses affecting the crop productivity based on minimum datasets, including but not restricted to average yield at field scale

and biomass measurements in selected locations. This approach is oriented to operational applications where the unique datasets available are the average yield at field scale and the temporal evolution of the reflectance data at pixel scale. The initial results are applied in water limited areas or growing seasons, where the water stress is the main factor limiting the crop productivity. The first step is to calibrate the soil water balance at field scale and for each field in terms of the average total available water which explain average yield measured in the field if the evolution of the mean value of T_{pot} at field scale is considered. The second step is to develop a function relating TAW and T_{pot} so that the average of the yield modelled for each pixel is equal to the average at field scale. In this work, we assume that the function TAW vs. T_{pot} is linear but further approaches can be developed. Under these assumptions, the values of the slope and interception for the function TAW vs. T_{pot} can be obtained only selecting the value of TAW for the minimum value of T_{pot}. The result of the calibration methodology is a map of TAW at the scale of the pixel analyzed. This map can be used for the implementation of the soil water balance model at pixel scale and can be evaluated in different growing seasons.

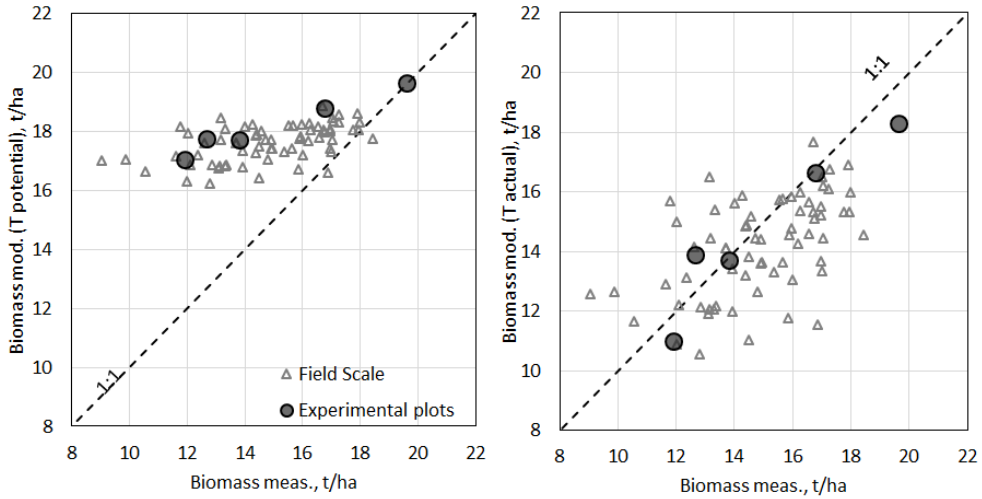

Figure 4-7. Comparison of measured and modelled biomass at the scale of field scale and experimental plots considering “non limiting conditions” (left) and considering water stress (right).

4.1.4.3 Results of the variable rate fertilization experiments

Based on the results of the field experiments already presented, we evaluate the results of VR and homogeneous applications of nitrogen fertilizer. The results of the experiment are analyzed in terms of yield, yield quality and efficiency. Further analysis will consider the environmental advantages of the proposed approach. In essence, the comparisons presented here referred to one crop (wheat) and two field experiments, the ongoing analysis try to evaluate the performance of the VR in fields with additional limitations such as water limited managements. In general terms, the application of VR fertilization promoted the crop productivity in less than 8% with respect to the homogeneous management but without increasing the average fertilization dose. In addition, the increase was consistent across fields and growing seasons and the application of the VR fertilization resulted in better crop performance in terms of N uptake and N efficiency.

The advantage of VR over the homogeneous practice usually used by the farmer was the increase of the yield in the more productive areas as consequence of the increasing fertilization doses. Equally, the less productive areas react positively to the increasing nitrogen doses (see Table 4.4 and 4.5). However, the increases in yields in the less productive areas was lower in comparison to the increment registered in the

high productive areas. In consequence the results averaged for both homogeneous and positive variable rate treatments clearly indicate the relative advantage of this methodology in the monitored fields. It should also be noted that the increment of the land productivity was obtained under different doses of fertilization, since the average total amounts applied in 2015 and 2016 differed in about a 25%. Further analysis will consider other benefits of the VR applications, paying special attention to the reduction of the nitrogen leaching risk as consequence of an excess of mineral nitrogen in the soil.

Table 4-4. Comparison of variable rate to homogeneous fertilization in the field 1.

		Low Fert.	Med. Fert.	High Fert.
Locations	Low Prod.	1^{+}	4^{*}	6^{-}
	Medium Prod.		2^{+*}	
	High Prod.	7^{-}	5^{*}	3^{+}
Yield Kg/ha	Low Prod.	9030	9272	9663
	Medium Prod.		8359	
	High Prod.	8570	9491	10199
N uptake. Kg/ha	Low Prod.	237	246	269
	Medium Prod.		220	
	High Prod.	221	246	282
N efficiency	Low Prod.	1.13	0.96	0.89
	Medium Prod.		0.86	
	High Prod.	1.05	0.96	0.93
Grain/N appli. Kg/Kg	Low Prod.	42.80	36.08	31.89
	Medium Prod.		32.53	
	High Prod.	40.62	36.93	33.66
Average	**Yield (Kg/ha)**	**N uptake (Kg/ha)**	**N efficiency**	**Grain/N appli. (Kg/Kg)**
VR +	9196	247	0.97	36.33
Homogeneous	9041	238	0.93	35.18
VI -	8865	237	0.93	35.01

+: Positive variable rate treatment. *: Homogeneous treatment. -: Negative variable rate treatment

Table 4-5. Comparison of variable rate to homogeneous fertilization in the field 2.

		Low Fert.	Med. Fert.	High Fert.
Locations	Low Prod.	1^{+}	4^{*}	
	Medium Prod.		2^{+*}	
	High Prod.		5^{*}	3^{+}
Yield Kg/ha	Low Prod.	6512	6946	
	Medium Prod.		7228	
	High Prod.		7576	9029
N uptake Kg/ha	Low Prod.	172	198	
	Medium Prod.		209	
	High Prod.		222	274
N efficiency	Low Prod.	1.03	0.91	
	Medium Prod.		0.96	
	High Prod.		1.02	1.07
Grain/N appli. Kg/Kg	Low Prod.	39.00	31.86	
	Medium Prod.		33.15	
	High Prod.		34.75	35.13
Average	**Yield (Kg/ha)**	**N uptake (Kg/ha)**	**N efficiency**	**Grain/N appli. (Kg/Kg)**
VR +	7590	218	1.02	35.76
Homogeneous	7250	210	0.96	33.26

+: Positive variable rate treatment. *: Homogeneous treatment

4.1.5 Yiels potential (2)

Results are displayed in the Table 4.6. They have shown a little improvement in term of Nitrogen use efficiency

Table 4-6. Comparison of the results between uniform and variable rate fertilisation

Variant	Avg. Yield (*t/ha*)	N Apllied (*kg N/ha*)	N Efficiency (*kg grain/kg N*)	N Efficiency (*differences in %*)
Trial – UNI	6.6	118	56	100
Trial – VAR	6.9	115	60	108
Whole field – UNI	6.5	118	55	100
Whole field – VAR	6.7	113	59	108
Whole field	6.6	116	57	

4.1.6 Yield potential (3)

Table 4.7 summarizes the N amounts and the fertilisation strategy applied for one commercial plot in one operational case. The VRA maps are shown in Figure 4.8. Figure 4.9 shows the results of the yield monitoring (obtained from the farmer at the harvest), the yield map that was obtained at the end of the season knowing the average yield of the field (UCLM) and the yield potential map at the time of the first fertilisation. Figure 4.10 shows the scatterplot between the yield potential map (long-term version using 2016 and 2017 S2 data) and the yield monitoring. Figure 4.11 shows a comparison between the Yara N-Sensor and the yield potential map.

Table 4-7. Commercial plot experiment

FERTILIZATION		
Field name	Tiergarten	
Crop type	Winter wheat	
Field size	18 ha	
Comments	Strategy: more fertilizer on more productive zones, less fertilizer on less productive zones	
Fertilization activity		
Date	**Amount**	**Type of fertilizer**
02.03.2017	44 kgN /ha uniform application	Ammonium sulphate nitrate 25%N
02.05.2017	33 kg/ha N average, 10kg/ha N minimum, 80 kg/ha N maximum	Calcium ammonium nitrate 27% N

29.05.2017	44 kg/ha average, 10kg/ha N minimum, 80 kg/ha N maximum	Urea 46%N

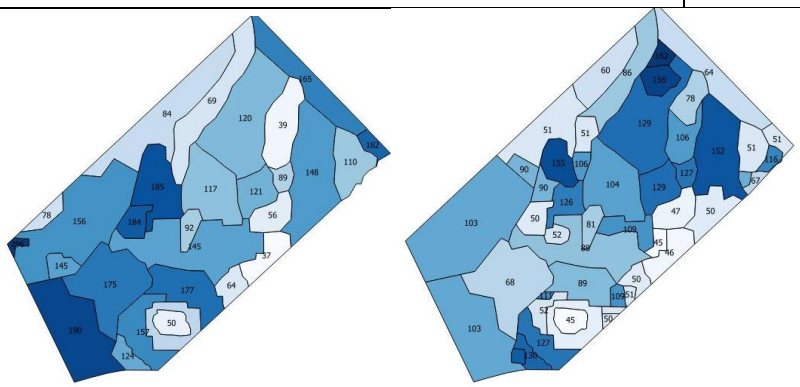

Figure 4-8. First (left, 02.05.2017) and second (right, 29.05.2017) Variable Rate Application (VRA) maps based on most recent Sentinel-2 yield potential maps produced at the time of the fertilisation application.

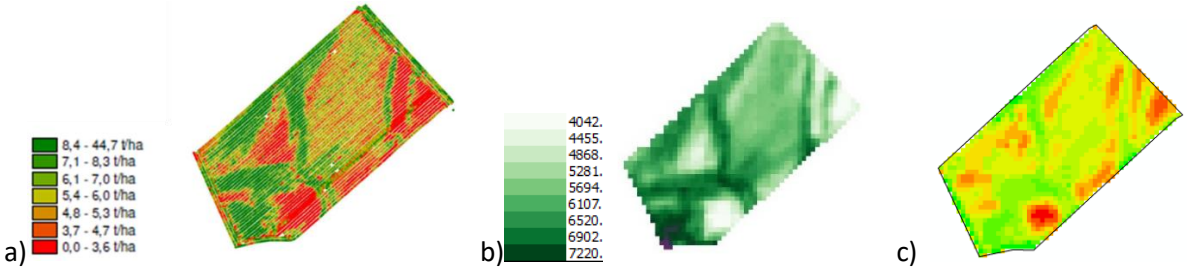

Figure 4-9. a: Field yield monitoring (obtained from the farmer); b: S-2 yield mapping (obtained at the end of the season knowing the average yield of the field – credit: UCLM); c: yield potential map at the time of the first fertilisation.

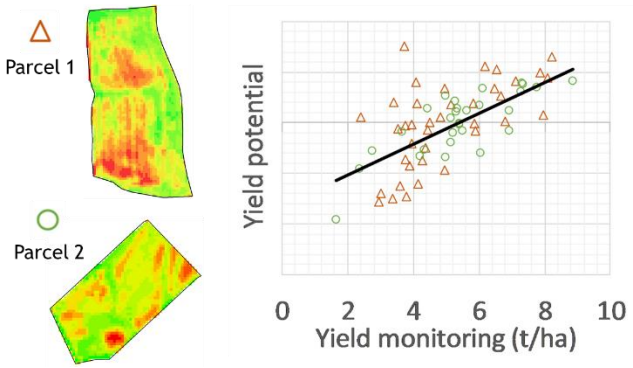

Figure 4-10. Satellite-based yield potential estimation vs yield monitoring for two parcels.

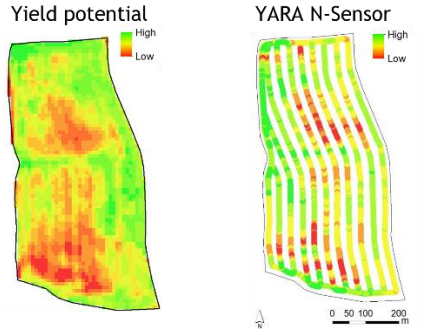

Figure 4-11. Yield potential vs biomass sampled by the Yara N-Sensor.

Live demo of the application

https://ivfl.maps.arcgis.com/apps/Cascade/index.html?appid=3b8fd1fd148a48ed8663a92009f89bd4#&preview

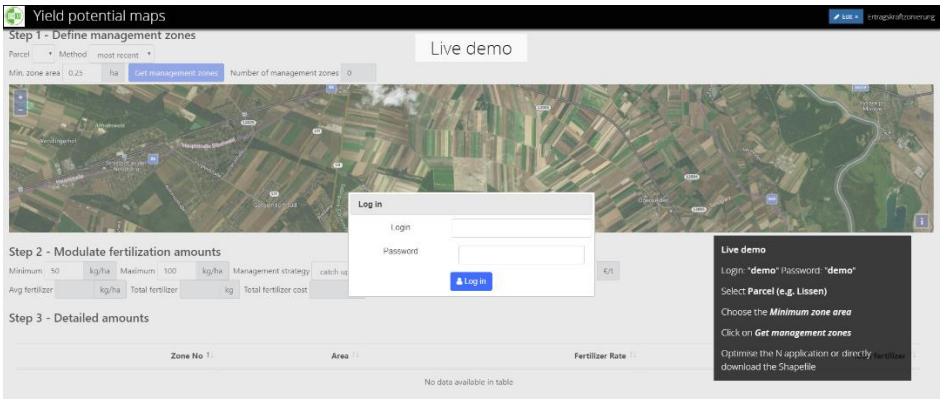

4.1.7 Crop model approach (INRA : Tarascon)

In Tarascon, on the 2nd (04/03/2016) and 3rd application (08/04/2016), fertilizer applied as calcium ammonium nitrate (CAN) using a commercial fertilizer spreader (model X40+, Sulky), linked to a GPS guided tractor. The GPS was fed with the spatialized N recommendations provided by the STICS simulations. As mentioned in the paragraph 3.7.4.4., the VRT approach was only applied to a small part of the field (= 82 grid cells), while the remaining part was fertilized according to a conventional average field N balance (Figure 4.12 and Figure 4.13).

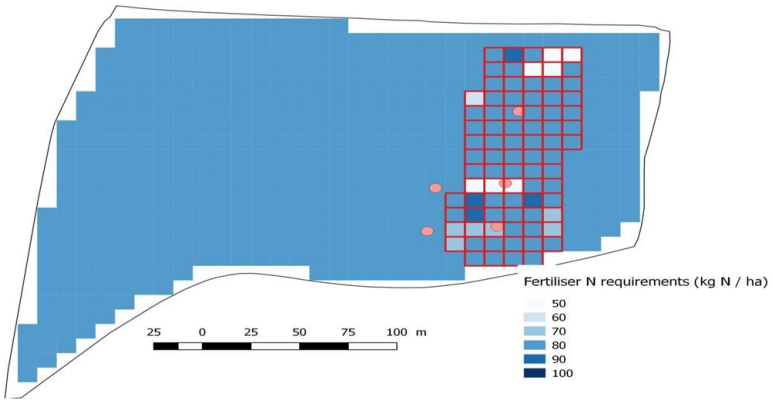

Figure 4-12. Fertiliser N recommendation map calculated for the 2nd application (04/03/2016) on the Tarascon field

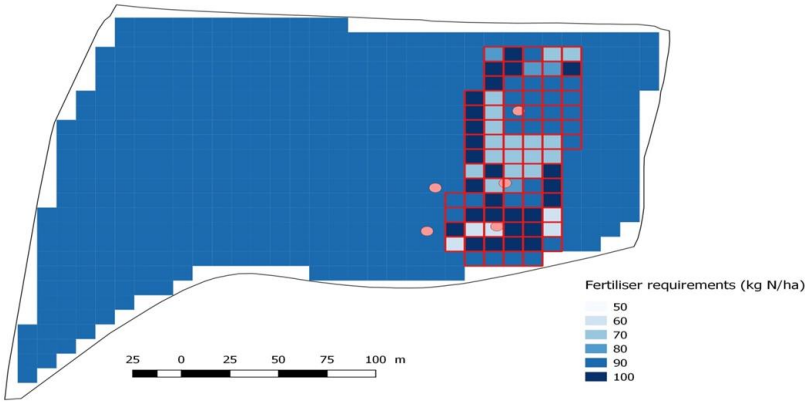

Figure 4-13. Fertiliser N recommendation map calculated for the 3rd application (08/04/2016) on the Tarascon field

To assess the impact of the VRT approach on yields, protein content and soil residual NO_3-N at harvest, in the Tarascon site, the three variables were simulated until harvest using observed weather data and inverted parameters such as soil water storage capacity (WSC) and sowing density. Results from inversions and calculated N recommendations for the five plots set up in the field are given in Table 4.8.

Table 4-8. Results from STICS inversion and calculation of fertilizer N recommendation for the five observation plots

Plot	Fertilization approach	Inverted soil WSC* (mm)	Sowing density (seeds m^{-2})	N recommendation	
				2nd application (kg N ha^{-1})	3rd application (kg N ha^{-1})
E3050	VRT	254 (225)	260	80	90
O30	Field N balance	254 (214)	340	80	90
E30	VRT	157 (158)	220	50	80
O	Field N balance	269 (267)	320	80	90
E	VRT	269 (252)	320	70	60

* in bracket are given the estimation from texture observation and pedotransfer function

For the simulations, plant parameters were taken from an existing STICS default variety (cv. Lloyd) as such variety was identified as quite similar to the actual one in place (cv. Pastadou).The ability for the model, parameterized as such, to reproduce observed yields and soil NO_3-N content at harvest was quite variable depending on plots (Table 4.9). The model underestimated the protein content in the grain, particularly in low productivity areas (Table 4.9).

Comparing both the “VRT approach” and the “average field N balance” scenarios through their simulation on the VRT-treated plots (Table 4.9) indicates only little effect of the VRT approach on simulated yields, but a possible increase in the gross margin for low productivity areas (e.g. plot E30) due to savings in fertilizer costs.

Table 4-9. Comparison between the "VRT approach" and the "average field N balance" scenarios. Both scenarios were compared for the VRT-treated plots (E3050, E30 and E). Simulated results for the "field N balance"-treated plots (O30, O) and field observations are given for comparison.

Plot	N fertilization	Yield (t ha^{-1})	Protein content (%)	Calculated gross margin (€ ha^{-1})	Soil NO_3-N content at harvest (kg N ha^{-1})
E3050	**Simul. VRT**	**6.98**	**10.1**	**1269**	**54.9**
	Simul. field N balance	6.98	10.1	1269	58.3
	Obs.	4.10	13.4	912	53.5
O30	Simul. VRT	-	-	-	-
	Simul. field N balance	**7.53**	**12.1**	**1116**	**52.5**
	Obs.	6.00	13.7	1151	61.3
E30	**Simul. VRT**	**4.34**	**9.9**	**821**	**54.5**
	Simul. field N balance	4.30	11.2	756	62.8
	Obs.	4.64	15.1	925	75.9
O	Simul. VRT	-	-	-	-
	Simul. field N balance	**7.28**	**11.5**	**1820**	**59.1**
	Obs.	7.29	12.5	1719	43.2
E	**Simul. VRT**	**6.92**	**8.5**	**1731**	**40.7**
	Simul. field N balance	7.00	8.9	1752	60.7
	Obs.	5.57	13.3	1650	68.8

4.2 Benchmarking

Three methods were compared:

- The SI approach (2.1) (AUA method). Three variants were considered
  - Without zoning (meaning that a single yield objective was applied for the field) and without a cut off function (AUAnotcut)
  - Without zoning but with the cut of function (AUAwithcut)
  - With zoning to better take into account the different yield potentials derived from the soil water storage capacity (AUAzone).
- UCLM recommendation (2.4) based on yield potential computed using the S2A data of year 2016 (a historical year should be taken but this was not possible with S2A launched in 2016) (INRA).
- The INRA recommendation (2.7), based on the use of the STICS crop model (INRA)

The fertilization map are given in the following Figures 4.14-4.18:

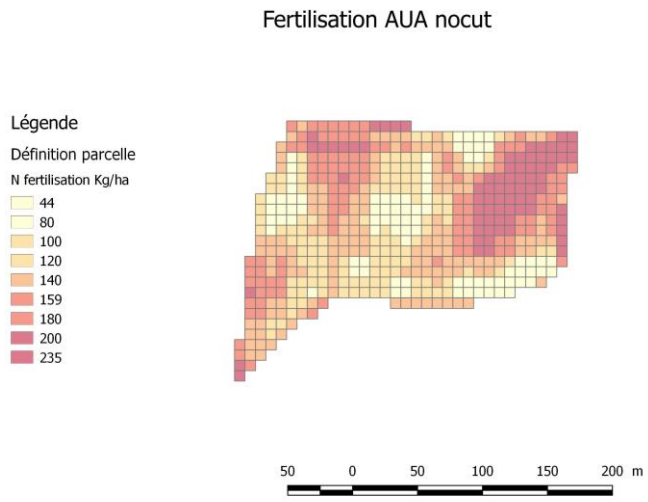

Figure 4-14. fertilization map obtained by the AUAnocut method

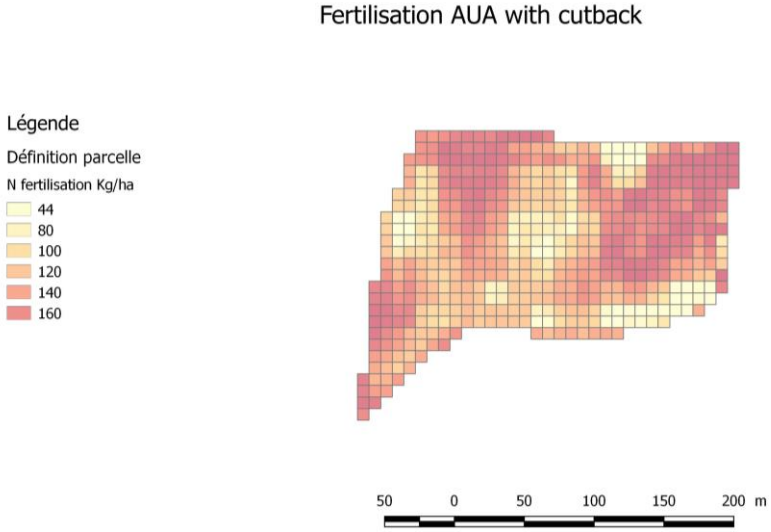

Figure 4-15. Fertilisation map with the AUAwithcut method

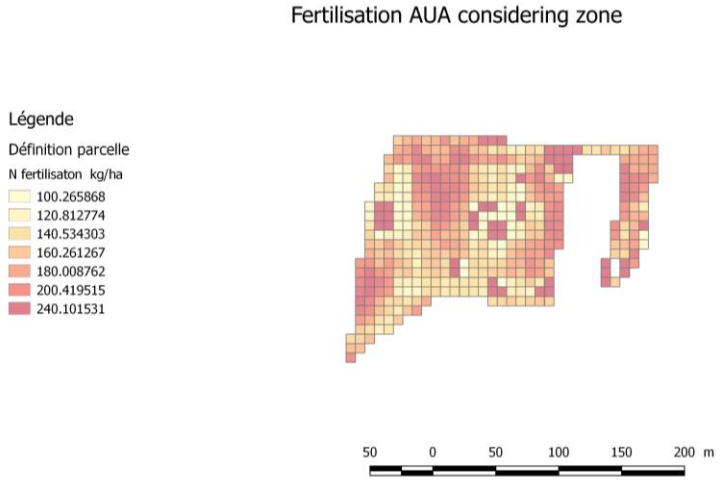

Figure 4-16. Fertilisation map with the AUAzone method

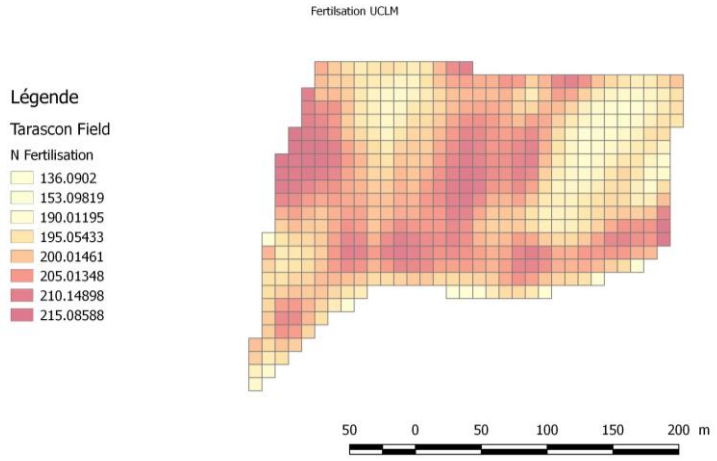

Figure 4-17. fertilization map obtained by the UCLM method

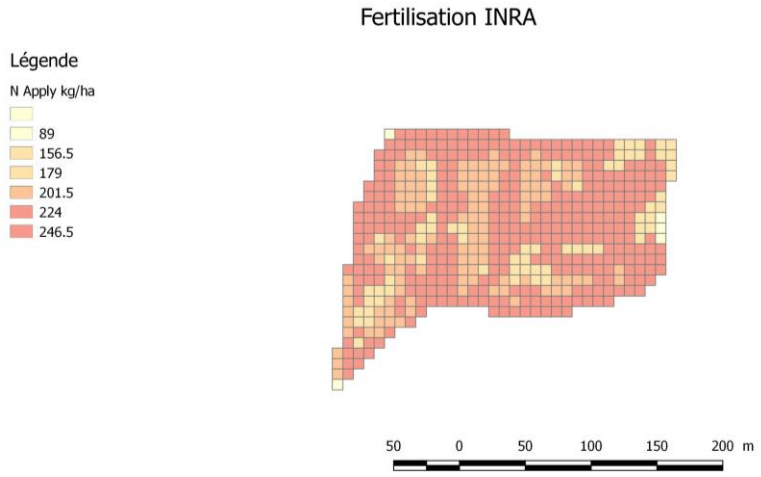

Figure 4-18. Fertilisation map with the INRA method

In the previous Figures we can see clearly that the methods led to very different patterns and very different range of recommendations (see Table 4.10). For instance UCLM proposed a small range of fertilization recommendation while it was much larger with AUA methods. On the other hand, this latter will lead to very low field average fertilization. The patterns between the AUA methods and UCLM are clearly the opposite. This can be explained by the method rationale which recommend more fertilization where the yield potential is high (corresponding in fact to the plant development of the considered year, since the yield potential was established using the same year as mentioned before (Fig 3.6)) whereas the AUA method proposed an opposite approach by recommending low fertilization when the plant is well developed. Such an approach is valid if there was no external source of variability. In the Tarascon field this was not the case since a large variability in texture was observed inducing a large range of water storage capacity (from 100 to 260 mm). An approach by zone was then applied, which led to spatial pattern less correlated to the vegetation development at the beginning of the crop season (Fig 4.18). Concerning the UCLM approach, the use of historical years would have led to different spatial patterns since part of the 2016 variability was affected by the quality of the crop installation (Fig 3.6). The spatial patterns of the INRA

method is very different from the other since it take into account both the soil map determined using historical data and crop installation development. The combination of the two factors led to N fertilization patterns that differed to that of foliar development in 2016 (see Fig 4.19)

Table 4-10. statistics at the field level of the N fertilization recommendation (Kg/ha).

	UCLM	INRA	AUAnocut	AUAwithcut	AUAzone
Mean	200	212	137	133	156
Min	136	89	44	44	44
max	216	247	235	179	240
Std	8	24	42	37	44

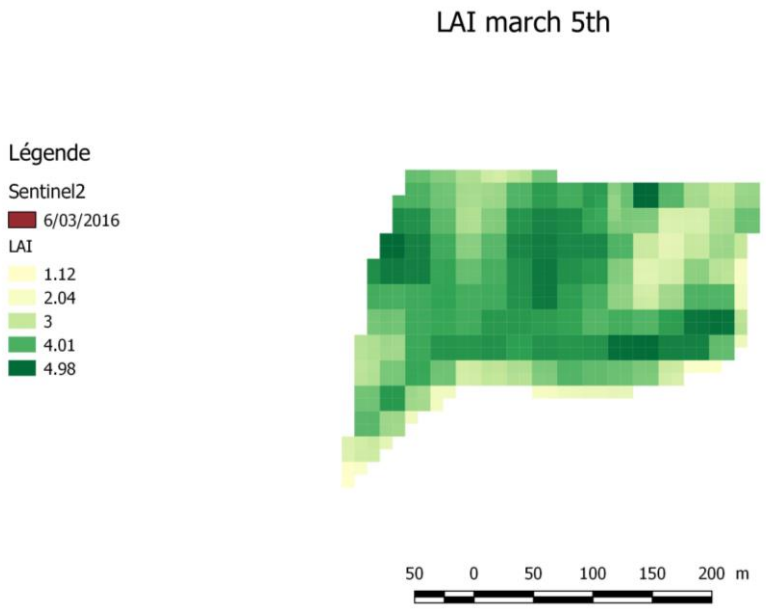

Figure 4-19. LAI index at the moment of the second N fertilization

The results of the simulation results are displayed in Table 4.11. Two treatments were added: Ref corresponded to a homogeneous dose determined by the farmers using a nitrogen balance method while N44 was a low homogeneous nitrogen application with 3 applications of 44kg/ha. NUE was the ratio of Yield by the applied Nitrogen for fertilization. N losses corresponded to the sum of leaching and N soil content at harvest. The comparison has shown very small losses. The gross margin was computed by subtracting to the yield revenue (200€/t) the cost of the Nitrogen (1.194 € per kilogram of applied N). As the variability in protein content was low, we did not take it the yield revenue as well as environmental cost of Nitrogen fertilization.

Table 4-11. Summary of the simulator results at the field scale

	ref	N44	UCLM	INRA	AUAnocut	AUAwithcut	AUAzone
N apply (mean Kg/ha	214	132	200	211	137	133	155
Yield (t/ha)	8.44	7.50	8.15	8.41	7.46	7.42	7.79
Protein (%)	13	11	12	13	11	11	12

N Leaching (Kg/ha)	1	1	1	1	1	1	1
N soil at harvest (Kg/ha)	7	2	9	8	4	3	3
Nitrogen Use efficiency (NUE) : Yield(Kg)/Napplied (Kg)	39.4	56.8	40.8	39.7	54.4	56.0	50.0
Gross Margin (€/ha)	1432	1343	1392	1428	1329	1325	1372
N Losses (Kg/ha)	8	3	10	9	5	4	4

The range of revenue is about 100 €/ha according to the strategy. This give an idea of the economic effect we can expect by applying different fertilization map. Using our economical inputs, the benefit is strongly linked to the average Nitrogen application. This is seen in the Figure 4.20

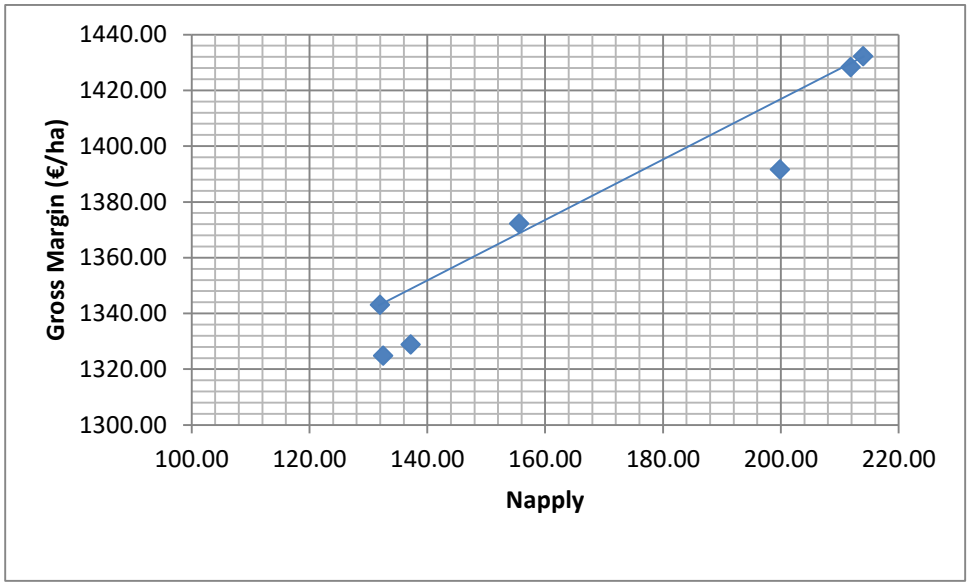

Figure 4-20. Average gross margin at the scale of the field as a function to the average N application obtained for the different methods.

The linear relationship relates the two homogeneous cases. It tells us that the gross margin is the highest with large fertilization rate. However the relative position of the points is a way of appreciating the benefit of the spatialized fertilization recommendation. In the present case, it show that the recommendation by the UCLM and UAU without zone have a negative impact with a loss of about 20€/ha. This was not the case with AUA zoning method and INRA method which gave similar results than the homogeneous cases. However, our results have some limitations that has to be considered:

- **Different climate** would lead to different results. 2016 was a moderately dry year and a wet or a very dry year might give very different pictures. The simulator has to take this into account by providing statistics based on simulation made with a range of possible climates
- If the **heterogeneity of the field** was large, pixel with soil having a low water storage capacity only represent a small fraction of the field, most of it having favorable soils. A more balance situation between good and bad soils will probably advantage spatially variable N application.

- The **simulator and the INRA method** used the same crop model giving an advantage to that method. The use of another crop model as EPIC for the evaluation will be fairer for the comparison between methods.

5 Conclusions

In the project several approaches for providing fertilization map were developed based on remotely sensed information. Two distinct approaches can be distinguished:

The use of remote sensing to detect N shortage and then adapt the fertilization to balance such a lack of N. This hold for the SI method (2.1) as well as those based on NNI (2.2 and 2.3). However, with this latter we did not go up to the decision and we remained with a generic information that has to be further used by a decision making process.

The use of remote sensing to establish the yield potential and thus adapt the fertilization to match the actual needs. The evaluation of the yield potential was done either simply by integrating historical LAI data (2.5 and 2.6), by considering biomass production that involves both the crop coefficient (Ks) through the NDVI dynamic (2.4) or by considering the sources in yield potential variability explicitly (soil properties as the organic matter or the water storage capacity) using a crop model (2.7). With yield potential approaches, the in season variability due to actual conditions (initial nitrogen or crop installation variability) can be addressed in order to modulated the yield potential by making a Nitrogen balance (2.4) or by considering these sources of variability in the crop model (2.7). In that case, the variability is established by inverting the model using the early satellite images.

Operational implementation : the SI method have shown some limitations when a zoning was not taken into account. This means that the method has to be combined with a yield potential approach. Such a combination has to be further developed or by implementing the other methods developed in the project. The NNI approaches still need a decision framework before being fully operational. The yield potential approaches based on vegetation dynamic (2.4, 2.6) are now operational, but need agronomic knowledge to scale the decisions. In 2.6 this is left to the farmer. The crop model approach is promising but still need developments to industrialize the recommendation process since a lot of processing is required to make the different inversion to grasp the permanent variability feature (soil properties, variety properties) as well the on season conditions.

The benchmarking was done on a single field and need to be replicated on the different fields in order to better evaluate the different methods. Moreover the simulator used to the benchmark has to be extended to another crop model and has to better account the climate variability that will have an impact on the results.

6 References

Allen, R. G., Raes, D., & Smith, M. (1998). Crop evapotranspiration: Guidelines for computing crop

requirements. *Irrigation and Drainage Paper No. 56, FAO, Rome, Italy*.

Asrar, G., Fuchs, M., Kanemasu, E. T., & Hatfield, J. L. (1984). Estimating Absorbed Photosynthetic Radiation and Leaf Area Index from Spectral Reflectance in Wheat. *Agronomy Journal*, *76*, 300–306.

Bastiaanssen, W., Allen, R. G., Droogers, P., D'Urso, G., & Steduto, P. (2007). Twenty -five years modelng irrigated and drained soils: State of the art. *Agricultural Water Management*, *92*, 111–125.

Bausch, W. C. (1993). Soil background effects on reflectance-based crop coefficients for corn. *Remote Sensing of Environment*, *46*, 213–222.

Benton Jones J, Wolf B & Mills H (1991). Plant analysis handbook: a practical sampling, preparation, analysis, and interpretation guide. Athens, Georgia: Micro-Macro Publishing Inc.

Biggs, G.L., T.M. Blackmer, T.H. Demetriades-Shah, K.H. Holland, J.S. Schepers, and J.H. Wurm. 2002. Method and apparatus for real-time determination and application of nitrogen fertilizer using rapid, non-destructive crop canopy measurements. U.S. Patent 6,393,927. 28 May 2002.

Brisson N., Mary B., Ripoche D., et al, 1998 - STICS: a generic model for the simulation of crops and their water and nitrogen balances. I. Theory and parameterization applied to wheat and corn. Agronomie, 18(5–6):311–346.

Buis, S, Wallach, D, , Guillaume, S, Varella, H, Lecharpentier, P, Launay, M, Guérif, M, Bergez, JE, and Justes E , 2011. The STICS crop model and associated software for analysis, parameterization and evaluation. In "Methods of introducing system models in field research » , Ahuja L., R., and Ma, L., Editors, ASA-CSSA-SSSA, ISBN 978-0-89118-180-4, 450 pp.

Calera, A., González-Piqueras, J., & Melia, J. (2004). Monitoring barley and corn growth from remote sensing data at field scale. *International Journal of Remote Sensing*, *25*(1), 97–109.

Chen, P., D. Haboudane, N. Tremblay, J. Wang, P. Vigneault, and B. Li, (2010). "New spectral indicator assessing the efficiency of crop nitrogen treatment in corn and wheat," *Remote Sens. Environ.*, vol. 114, no. 9, pp. 1987–1997.

Cilia, C. C. Panigada, M. Rossini, M. Meroni, L. Busetto, S. Amaducci, M. Boschetti, V. Picchi, and R. Colombo, (2014), "Nitrogen status assessment for variable rate fertilization in maize through hyperspectral imagery," *Remote Sens.*, vol. 6, no. 7, pp. 6549–6565.

COLNENNE, C. J. M. MEYNARD, R. REAU, E. JUSTES, and A. MERRIEN, "Determination of a Critical Nitrogen Dilution Curve for Winter Oilseed Rape," *Ann. Bot.*, vol. 81, no. 2, pp. 311–317, Feb. 1998.Dobermann A, Ferguson R, Hergert G, Shapiro C, Tarkalson D, Walters DT & Wortmann C (2006). Nitrogen response in high-yielding corn systems of Nebraska, Proc. Great Plains Soil Fertility Conf. (Denver CO) Vol 11. Potash & Phosphate Inst., Brookings, SD, pp. 50-59.

Campos, I., González, L., Villodre, J., Calera, M., Campoy, J., Jiménez, N., et al. (2017). Mapping within-field biomass variability: a remote sensing-based approach. *Advances in Animal Biosciences*, *8*(02), 764–769. doi:10.1017/S2040470017000139

Campos, I., González-Gómez, L., Villodre, J., González-Piqueras, J., Suyker, A., & Calera, A. (2018). Remote sensing based crop biomass with water or light-driven crop growth models in wheat commercial fields. *Field Crop Research*.

Campos, I., Neale, C., Suyker, A., Arkebauer, T., & Gonçalves, I. (2017). Reflectance-based crop coefficients REDUX: for operational evapotranspiration estimates in the age of high producing hybrid varieties. *Agricultural Water Management*, *187*, 140–153.

Choudhury, B. J. (1987). Relationships between vegetation indices, radiation absortion, and net photosyntesis evaluated by a sensivity analysis. *Remote Sensing of Environment*, *22*, 209–233.

D'Urso, G., Richter, K., Calera, A., Osann, M. A., Escadafal, R., Garatuza-Pajan, J., et al. (2010). Earth

Observation products for operational irrigation management in the context of the PLEIADeS project. *Agricultural Water Management*, *98*(2), 271–282.

Doorenbos, J., & Kassam, A. H. (1979). *Yield response to water*. *Irrigation and Drainage Paper N^{o} 33*. Rome: Food and Agriculture Organization of the United Nations.

Doorenbos, J., & Pruitt, W. O. (1977). Guidelines for predicting crop water requierements. *Irrigation and Drainage Paper No. 24, FAO, Rome, Italy*.

Fischer, R., & Maurer, R. (1978). Drought resistance in spring wheat cultivars. I. Grain yield responses. *Australian Journal of Agricultural Research*, *29*(5), 897. doi:10.1071/AR9780897

Glenn, E. P., Neale, C. M. U., Hunsaker, D. J., & Nagler, P. L. (2011). Vegetation index-based crop coefficients to estimate evapotranspiration by remote sensing in agricultural and natural ecosystems. *Hydrologycal processes*, *25*, 4050–4062.

González-Dugo, M. P., & Mateos, L. (2008). Spectral vegetation indices for benchmarking water productivity of irrigated cotton and sugarbeet crops. *Agricultural Water Management*, *95*(1), 48–58.

Guérif, M., Houlès, V., Makowski, D., Lauvernet, C., 2007. Data assimilation and parameter estimation for precision agriculture using the crop model STICS. In: "Working with Dynamic Crop Models", Wallach,D., Makowski, D., and Jones, J.W. (eds), pp 395-402.

Holland KH & Schepers JS (2010). Derivation of a variable rate nitrogen application model for in-season fertilization of corn. Agronomy Journal, 102: 1415-1424.

Holland KH & Schepers JS (2011). Active-crop sensor calibration using the virtual reference concept. P. 469-479. In J.V. Stafford (ed.) Precision Agriculture 2011. Czech Centre for Science and Society, Prague, Czech Republic.

Houlès, V., Guérif, M., Mary, B., Machet, J.M., Moulin, S., Beaudoin, N., 2005. A tool devoted to recommend spatialized nitrogen rates at the field scale, based on a crop model and remote sensing observations assimilation. Precision Agriculture '05, J.V. Stafford (ed.).

Houlès, V. M. Guérif, and B. Mary, (2007) "Elaboration of a nitrogen nutrition indicator for winter wheat based on leaf area index and chlorophyll content for making nitrogen recommendations," *Eur. J. Agron.*, vol. 27, no. 1, pp. 1–11.

Justes, E., Jeuffroy, M., & Mary, B. (1997). Wheat, Barley and Durum Wheat. In G. Lemaire (Ed.), *Diagnosis of the Nitrogen Status in Crops* (pp. 73–91). Berlin, Heidelberg: Springer-Verlag.

Kemanian, A. R., Stöckle, C. O., Huggins, D. R., & Viega, L. . (2007). A simple method to estimate harvest index in grain crops. *Field Crops Research*, *103*(3), 208–216. doi:10.1016/j.fcr.2007.06.007

Lemaire, G. M.-H. Jeuffroy, and F. Gastal, (2008) "Diagnosis tool for plant and crop N status in vegetative stage: Theory and practices for crop N management," *Eur. J. Agron.*, vol. 28, no. 4, pp. 614–624.

Lobell, D. B., Ortiz-Monasterio, J. I., Sibley, A. M., & Sohu, V. S. (2013). Satellite detection of earlier wheat sowing in India and implications for yield trends. *Agricultural Systems*, *115*, 137–143. doi:10.1016/j.agsy.2012.09.003

Lukaszyk S (2004). A new concept of probability metric and its applications in approximation of scattered data sets. Computational Mechanics (2004) 33: 299.

Meisinger JJ & Randall GW (1991). Estimating nitrogen budgets for soil-crop systems. In: RF Follett et al. (Eds.), Managing nitrogen for groundwater quality and farm profitability. Madison, WI: SSSA. pp. 85-124.

Meisinger JJ, Schepers JS & Raun WR (2008). Crop nitrogen requirement and fertilization. In: Nitrogen in agricultural systems, Agronomy Monograph 49. Madison, WI: ASA. pp. 563-612.

Monteith, J. L. (1972). Solar Radiation and Productivity in Tropical Ecosystems. *Journal of applied ecology*, *9*,

747–766.

Moreno, A., Maselli, F., Gilabert, M. A., Chiesi, M., Martínez, B., & Seufert, G. (2012). Assessment of MODISimagery to tracklight-use efficiency in a water-limited Mediterranean pine forest. Remote Sensing of Environment. *Remote Sensing of Environment*, *123*, 359–367.

Neale, C., Bausch, W., & Heerman, D. (1989). Development of reflectance-based crop coefficients for corn. *Transactions of the ASAE*, *32*(6), 1891–1899.

Perry, C., Steduto, P., Allen, R. G., & Burt, C. M. (2009). Increasing productivity in irrigated agriculture: Agronomic constraints and hydrological realities. *Agricultural Water Management*, *96*(11), 1517–1524.

Peterson, T.A., T.M. Blackmer, D.D. Francis, and J.S. Schepers. 1993. Using a chlorophyll meter to improve N management. NebGuide G93–1171-A. Univ. of Nebraska Ext., Lincoln.

Pinter, P., Ritchie, J., Hatfield, J., & Hart, G. (2003). The Agricultural Research Service's remote sensing program: An example of interagency collaboration. *Photogrammetric Engineering and Remote Sensing*, *69*(6), 615–618.

Power JF & Schepers JS (1989). Nitrate contamination of groundwater in North America. Agric. Ecosyst. Environ. 26: 165-187.

Peterson, T.A., T.M. Blackmer, D.D. Francis, and J.S. Schepers. 1993. Using a chlorophyll meter to improve N management. NebGuide G93–1171-A. Univ. of Nebraska Ext., Lincoln.

Power JF & Schepers JS (1989). Nitrate contamination of groundwater in North America. Agric. Ecosyst. Environ. 26: 165-187.

Ritchie, J. T., Singh, U., Godwin, D. C., & Bowen, W. T. (1998). Cereal growth, development and yield. *Understanding options for agricultural production*, 79–98. doi:10.1007/978-94-017-3624-4_5

Sadras, V. O., & Connor, D. J. (1991). Physiological basis of the response of harvest index to the fraction of water transpired after anthesis: A simple model to estimate harvest index for determinate species. *Field Crops Research*, *26*(3-4), 227–239. doi:10.1016/0378-4290(91)90001-C

Sellers, P. J. (1987). Canopy reflectance, photosynthesis, and transpiration, II. The role of biophysics in the linearity of their interdependence. *Remote Sensing of Environment*, *21*(2), 143–183.

Sellers, P. J., Dickinson, R. E., Randall, D. A., Betts, A. K., Hall, F. G., Berry, J. A., et al. (1997). Modeling the exchanges of energy, water, and carbon between continents and the atmosphere. *Science*, *275*, 502–509.

Shepard D (1968). A two-dimensional interpolation function for irregularly-spaced data. Proc. ACM '68 Proc. of the 1968 23rd ACM national conference. pp. 517-524.

Schepers JS, Francis DD & Thompson MT (1989). Simultaneous determination of total C, total N, and 15N on soil and plant material. Communications Soil Science Plant Analysis, 20(9&10): 949-959.

Schepers, J. S., Francis, D. D., Vigil, M., & Below, F. E. (1992). Comparison of corn leaf nitrogen and chlorophyll meter readings. Communications in Soil Science and Plant Analysis, 23(17–20), 2173–2187.

Schledgel AJ, Dhuyvetter KC & Havlin JL (1996). Economic and environmental impacts of long-term nitrogen and phosphorus fertilization. J. Proc. Agric. 9: 114-118.

Sibley, A. M., Grassini, P., Thomas, N. E., Cassman, K. G., & Lobell, D. B. (2014). Testing remote sensing approaches for assessing yield variability among maize fields. *Agronomy Journal*, *106*(1), 24–32. doi:10.2134/agronj2013.0314

Sibson R (1980). A vector identity for the Dirichlet tessellation. Math Proc. Cambridge Philos. Soc. 87 (1980): 151-155.

Stafford, J. V., Ambler, B., Lark, R. M., & Catt, J. (1996). Mapping and interpreting the yield variation in cereal crops. *Computers and Electronics in Agriculture*, *14*(2-3), 101–119. doi:10.1016/0168-1699(95)00042-9

Stamatiadis S, Tsadilas C, Samaras V, Eskridge K & Schepers JS (2016). Nitrogen mass balance and N-use efficiency of Mediterranean cotton under varied levels of fertilization and deficit irrigation. European Journal of Agronomy 73:144-151.

Steduto, P., & Albrizio, R. (2005). Resource use efficiency of field-grown sunflower, sorghum, wheat and chickpea II. Water use efficiency and comparison with radiation use efficiency. *Agricultural and Forest Meteorology*, *130*, 269–281.

Steduto, P., Hsiao, T., Fereres, E., & Raes, D. (2012). FAO Irrigation and drainage paper 66. Crop yield response to water. *FAO Irrigation and Drainage Paper No.66*, (February 2016), 505.

Tanner, C. B., & Sinclair, T. R. (1983). Efficient water use in crop production: Research or Research? In W. R. J. and T. R. S. H.M. Taylor (Ed.), *Limitations to Efficient Water Use in Crop Production*. Madison, WI, USA. : Amer. Soc. Agron.

Varella, H, Guérif, M, Buis, S, 2010. Global sensitivity analysis measures the quality of parameter estimation: The case of soil parameters and a crop model. Environmental Modelling & Software, 25: 310–319.

Varvel, G.E., W.W. Wilhelm, J.F. Shanahan, and J.S. Schepers. 2007. An algorithm for corn nitrogen recommendations using a chlorophyll meter based sufficiency index. Agron. J. 99:701–706.

Verger, A., Vigneau, N., Chéron , C., Gilliot , JM., Comar, A., Baret, F.. Green area index from an unmanned aerial system over wheat and rapeseed crops. Remote Sensing of Environment, 152: 654-664.

Vouillot, M.-O., P. Huet, and P. Boissard, (1998) “Early detection of N deficiency in a wheat crop using physiological and radiometric methods,” *Agronomie*, vol. 18, no. 2, pp. 117–130.

Wiegand, C. L., & Richardson, A. J. (1990). Use of spectral vegetation indices to infer leaf area, evapotranspiration and yield: I. Rationale. *Agron. J.*, *82*, 623–629.

Zhao et al., New criticical Nitrogen curve based on leaf area index for winter wheat. Agronomy J.2014, 106 (2): 379-389